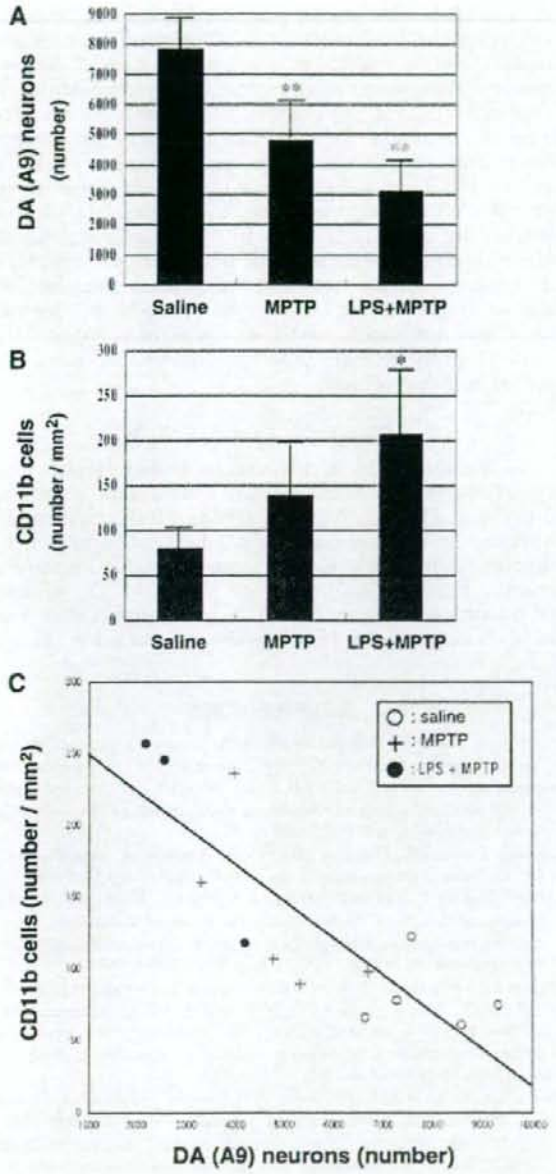

Fig. 5. Effects of microglial activation by LPS treatment on numbers of DA neurons and microglia in SN of 60-week-old (aged) mice treated with MPTP. **A:** Number of DA (A9) neurons in saline, MPTP, and LPS-MPTP groups. The number in the MPTP and LPS-MPTP groups was decreased significantly. **B:** Number of CD11b-immunopositive microglia in saline, MPTP, and LPS-MPTP groups. Severe microglial activation was observed in the LPS-MPTP group. Values represent the mean ± SD. $*P < 0.05$; $**P < 0.01$ vs. saline group (unpaired Student's *t*-test) ($n = 3$–5). **C:** Relationship between activated microglia and DA (A9) neurons in the SNc of MPTP-treated aged mice. An inverse correlation ($R = 0.81$) was observed between the two parameters when data for all three groups was plotted.

nificantly over those in the saline or MPTP group (IL-1β: 184% of the saline group, 207% of the MPTP group; and IL-6: 188% of the MPTP group, respectively).

The mRNA expressions of neurotrophic factors were also measured as their ratios to GAPDH by RT-PCR method. The mRNA expressions of NGF-β, BDNF, and NT-4/5 tended to decrease in the MPTP group, and these of the LPS-MPTP group were recovered to those of the saline group (Fig. 4B). As to the NT-3, the mRNA expression tended to most increase in LPS-MPTP group (Fig. 4B). However, statistical differences were not observed due to variations of the data.

Effects of Microglial Activation by LPS Treatment on the Number of Dopamine Neurons in Aged Mice Administered MPTP

Aged, 60-week-old male mice were pretreated with LPS to activate their microglia, and then given a single injection of MPTP. The number of DA (A9) neurons in the aged mice was decreased in the MPTP group (to 61% of the saline group); and that of the LPS-MPTP group was markedly decreased (to 40% of the saline group) by the single MPTP administration (Fig. 5A). The MPTP group of aged mice showed an increased number of activated microglia in their SNc; and in the LPS-MPTP group, the increase was statistically significant (Fig. 5B). The relationship between microglial activation and viability of DA (A9) neurons for the three groups of aged mice showed an inverse correlation ($R = 0.81$) (Fig. 5C).

DISCUSSION

In this study, we showed the possibility that microglia activated by treatment with LPS may have neurotrophic potential toward DA neurons in neonatal mice administered MPTP. TH activity and the levels of DA and DOPAC, as well as those of the pro-inflammatory cytokines IL-1β and IL-6, were elevated in the midbrain of LPS-MPTP-treated neonatal mice (Figs. 3,4). The cell viability of DA (A9) neurons was recovered in neonatal mice of the LPS-MPTP group compared with that for the MPTP group (Fig. 2). In contrast, the viability of these neurons in the aged mice dropped significantly by the same comparison (Fig. 5). These results may suggest that the activated microglia are different between neonatal and aged brains; i.e., the activated microglia in the neonatal brain may act for neuroprotection in MPTP-PD mice, whereas those in the same group of aged mice may be neurotoxic. Several results from cell culture systems in vitro indicate that activated microglia may act in a neuroprotective manner. The present study is the first in vivo one suggesting the neuroprotective effects of activated microglia on DA neurons in the SN of neonatal mice.

There are many reports indicating the neurotoxic effects of activated microglia especially in aged animals. Cultures of amyloid β-peptide (Aβ)-stimulated microglia

from aged rats were reported to show more evidence of toxicity than those from middle-aged or embryonic mice (Viel et al., 2001). Furthermore, MPTP neurotoxicity was greater in aged mice than in young mice, and was accompanied by age-related microglial activation (Sugama et al., 2003). These reports agree with the present findings that activated microglia in old animals play a toxic role. LPS treatment caused neurotoxic effects on DA neurons in various cell culture systems (Kim et al., 2000; Gayle et al., 2002; Gao et al., 2003) or by direct injection into the SN (Castano et al., 2002; Arai et al., 2004; Iravani et al., 2005). The degree of neuronal injury may depend on the concentration of LPS used for treatment. The neurotoxicity of microglia was increased by the production of TNFα by the cells in response to LPS stimulation (Sawada et al., 1989, 1995).

Activated microglia may produce not only neurotoxic effects, but also neuroprotective ones depending upon their environmental situation. The present results agree with the previous results of Imamura et al. (2003, 2005) and Sawada et al. (2006), who demonstrated the existence of toxic and neuroprotective subsets of activated microglia. Vilhardt et al. (2002) discovered a toxic change in microglia, from neuroprotection to neurotoxicity, by transfecting the cells with cDNA encoding HIV-1 Nef protein, indicating the conversion from a neurotrophic to a neurotoxic subtype of microglia. During aging a similar toxic change may be induced in the microglia of the brain.

On the other hand, the neurotrophic effects of microglial activation induced by LPS have also been found in several cell culture studies (Mallat et al., 1989; Miwa et al., 1997; Elkabes et al., 1998; Nakajima et al., 2001; Kramer et al., 2002). The neurotrophic effects of LPS may be explained by the fact that LPS induces the secretion of not only pro-inflammatory cytokines but also neurotrophic compounds. LPS stimulation increases the microglial secretion of NT-3, NT-4/5, NGF, and BDNF (Miwa et al., 1997; Elkabes et al., 1998; Nakajima et al., 2001). A rat model of spinal cord injury showed improvement in locomotor function by an LPS-elicited increase in the level of neuroprotective GDNF (Hashimoto et al., 2005). Plasminogen produced by LPS-treated microglia was reported to promote the development of DA neurons (Nakajima et al., 1992; Nagata et al., 1993b). Pro-inflammatory cytokines, such as TNFα, IL-1β, and IL-6, produced from activated microglia, are pleiotropic, and act for either neuroprotection or neurotoxicity.

Neuroprotective and neurotoxic effects of microglia in neonate and adult mice are possible explanation of the present results. However, cautious interpretation is required in considering the complexity of the present experimental condition. Because in our experiment, LPS treatment was carried out by systemic injection, microglial activation may occur in the entire brain. Although different effects of microglia in neonatal and adult mice are one probable explanation of the present results, the comparison between the changes observed in the neonatal and adult mice is very difficult, because many factors can affect the final outcome. Cells that respond directly to LPS are microglia, but we induced systemic inflammation. Thus, many cells, such as astrocytes, vascular endothelial cells, and in particular, T cells, may be involved. The sensitivity of DA neurons to MPTP is different depending on the age (Jarvis and Wagner, 1985; Ali et al., 1993). It is hard to judge whether the dosage of MPTP/LPS, we employed is appropriate to induce the exactly comparable effect to the neurons and microglia of both neonatal and adult mice. The present results showing microglial activation and protection by LPS against dopaminergic damage in the SN in neonatal mice and neurotoxic effect in aged mice suggest that most probably activated microglia in neonatal mice may act for neuroprotection.

ACKNOWLEDGMENTS

We thank Dr. S. Hashimoto (Fujita Health University, School of Medicine) for a discussion about statistics and Dr. K. Tsuchida (Fujita Health University, Institute for Comprehensive Medical Science) for his support of this work. Contract grant sponsor: Ministry of Health, Labor, and Welfare of Japan (M.S.); Ministry of Education, Culture, Sports, Science, and Technology of Japan (M.S.); Japan Health Sciences Foundation (M.S.).

REFERENCES

Aguirre JA, Cintra A, Hillion J, Narváez JA, Jansson A, Antonelli T, Ferraro L, Rambert FA, Fuxe K. 1999. A stereological study on the neuroprotective actions of acute Modafinil treatment on 1-methyl-4-phenyl-1,2,3,6-tetrahydropyridine-induced nigral lesions of the male black mouse. Neurosci Lett 275:215–218.

Ali SF, David SN, Newport GD. 1993. Age-related susceptibility to MPTP-induced neurotoxicity in mice. Neurotoxicology 14:29–34.

Arai H, Furuya T, Yasuda T, Miura M, Mizuno Y, Mochizuki H. 2004. Neurotoxic effects of lipopolysaccharide on nigral dopaminergic neurons are mediated by microglial activation, interleukin-1β, and expression of caspase-11 in mice. J Biol Chem 279:51647–51653.

Barger SW, Hörster D, Furukawa K, Goodman Y, Krieglstein J, Mattson MP. 1995. Tumor necrosis factors α and β protect neurons against amyloid β-peptide toxicity: evidence for involvement of a κB-binding factor and attenuation of peroxide and Ca^{2+} accumulation. Proc Natl Acad Sci U S A 92:9328–9332.

Batchelor PE, Liberatore GT, Wong JYF, Porritt MJ, Frerichs F, Donnan GA, Howells DW. 1999. Activated macrophages and microglia induce dopaminergic sprouting in the injured striatum and express brain-derived neurotrophic factor and glial cell line-derived neurotrophic factor. J Neurosci 19:1708–1716.

Bolin LM, Strychanska-Orczyk I, Murray R, Langston JW, Monte DD. 2002. Increased vulnerability of dopaminergic neurons in MPTP-lesioned interleukin-6 deficient mice. J Neurochem 83:167–175.

Cassarino DS, Fall CP, Swerdlow RH, Smith TS, Halvorsen EM, Miller SW, Parks JP, Parker WD Jr, Bennett JP Jr. 1997. Elevated reactive oxygen species and antioxidant enzyme activities in animal and cellular models of Parkinson's disease. Biochim Biophys Acta 1362:77–86.

Castano A, Herrera AJ, Cano J, Machado A. 2002. The degenerative effect of a single intra-nigral injection of LPS on the dopaminergic system is prevented by dexamethasone, and not mimicked by rh-TNF-α, IL-1β and IFN-γ. J Neurochem 81:150–157.

Chao CC, Hu S, Molitor TW, Shaskan EG, Peterson PK. 1992. Activated microglia mediate neuronal cell injury via a nitric oxide mechanism. J Immunol 149:2736–2741.

Elkabes S, DiCicco-Bloom EM, Black IB. 1996. Brain microglia/macrophages express neurotrophins that selectively regulate microglial proliferation and function. J Neurosci 16:2508–2521.

Elkabes S, Peng L, Black IB. 1998. Lipopolysaccharide differentially regulates microglial trk receptor and neurotrophin expression. J Neurosci Res 54:117–122.

Fisher J, Mizrahi T, Schori H, Yoles E, Levkovitch-Verbin H, Haggiag S, Revel M, Schwartz M. 2001. Increased post-traumatic survival of neurons in IL-6-knockout mice on a background of EAE susceptibility. J Neuroimmunol 119:1–9.

Franklin KBJ, Paxinos G. 1997. The mouse brain in stereotaxic coordinates. London: Academic Press.

Furuya T, Hayakawa H, Yamada M, Yoshimi K, Hisahara S, Miura M, Mizuno Y, Mochizuki H. 2004. Caspase-11 mediates inflammatory dopaminergic cell death in the 1-methyl-4-phenyl-1,2,3,6-tetrahydropyridine mouse model of Parkinson's disease. J Neurosci 24:1865–1872.

Gao HM, Hong JS, Zhang W, Liu B. 2003. Synergistic dopaminergic neurotoxicity of the pesticide rotenone and inflammogen lipopolysaccharide: relevance to the etiology of Parkinson's disease. J Neurosci 23:1228–1236.

Gayle DA, Ling Z, Tong C, Landers T, Lipton JW, Carvey PM. 2002. Lipopolysaccharide (LPS)-induced dopamine cell loss in culture: roles of tumor necrosis factor-alpha, interleukin-1beta, and nitric oxide. Brain Res Dev Brain Res 133:27–35.

Hashimoto M, Nitta A, Fukumitsu H, Nomoto H, Shen L, Furukawa S. 2005. Inflammation-induced GDNF improves locomotor function after spinal cord injury. Neuroreport 16:99–102.

Hirata Y, Kiuchi K, Nagatsu T. 2001. Manganese mimics the action of 1-methyl-4-phenylpyridinium ion, a dopaminergic neurotoxin, in rat striatal tissue slices. Neurosci Lett 311:53–56.

Hunot S, Boissiere F, Faucheux B, Brugg B, Mouatt-Prigent A, Agid Y, Hirsch EC. 1996. Nitric oxide synthase and neuronal vulnerability in Parkinson's disease. Neuroscience 72:355–363.

Imamura K, Hishikawa N, Sawada M, Nagatsu T, Yoshida M, Hashizume Y. 2003. Distribution of major histocompatibility complex class II-positive microglia and cytokine profile of Parkinson's disease brains. Acta Neuropathol 106:518–526.

Imamura K, Hishikawa N, Ono K, Suzuki H, Sawada M, Nagatsu T, Yoshida M, Hashizume Y. 2005. Cytokine production of activated microglia and decrease in neurotrophic factors of neurons in the hippocampus of Lewy body disease brains. Acta Neuropathol 109:141–150.

Iravani MM, Leung CCM, Sadeghian M, Haddon CO, Rose S, Jenner P. 2005. The acute and the long-term effects of nigral lipopolysaccharide administration on dopaminergic dysfunction and glial cell activation. Eur J Neurosci 22:317–330.

Jarvis MF, Wagner GC. 1985. Age-dependent effects of 1-methyl-4-phenyl-1,2,5,6-tetrahydropyridine (MPTP). Neuropharmacology 24:581–583.

Kramer BC, Yabut JA, Cheong J, JnoBaptiste R, Robakis T, Olanow CW, Mytilineou C. 2002. Lipopolysaccharide prevents cell death caused by glutathione depletion: possible mechanisms of protection. Neuroscience 114:361–372.

Kim WG, Mohney RP, Wilson B, Jeohn GH, Liu B, Hong JS. 2000. Regional difference in susceptibility to lipopolysaccharide-induced neurotoxicity in the rat brain: role of microglia. J Neurosci 20:6309–6316.

Koutsilieri E, Scheller C, Grünblatt E, Nara K, Li J, Riederer P. 2002. Free radicals in Parkinson's disease. J Neurol 249(Suppl):II/1–II/5.

Lehnardt S, Massillon L, Follett P, Jensen FE, Ratan R, Rosenberg PA, Volpe JJ, Vartanian T. 2003. Activation of innate immunity in the CNS triggers neurodegeneration through a Toll-like receptor 4-dependent pathway. Proc Natl Acad Sci U S A 100:8514–8519.

Liu J, Marino MW, Wong G, Grail D, Dunn A, Bettadapura J, Slavin AJ, Old L, Bernard CC. 1998. TNF is a potent anti-inflammatory cytokine in autoimmune-mediated demyelination. Nat Med 4:78–83.

Mason JL, Suzuki K, Chaplin DD, Matsushima GK. 2001. Interleukin-1β promotes repair of the CNS. J Neurosci 21:7046–7052.

Mallat M, Houlgatte R, Brachet P, Prochiantz A. 1989. Lipopolysaccharide-stimulated rat brain macrophages release NGF in vitro. Dev Biol 133:309–311.

McGuire SO, Ling ZD, Lipton JW, Sortwell CE, Collier TJ, Carvey PM. 2001. Tumor necrosis factor α is toxic to embryonic mesencephalic dopamine neurons. Exp Neurol 169:219–230.

Miwa T, Furukawa S, Nakajima K, Furukawa Y, Kohsaka S. 1997. Lipopolysaccharide enhances synthesis of brain-derived neurotrophic factor in cultured rat microglia. J Neurosci Res 50:1023–1029.

Mogi M, Harada M, Riederer P, Narabayashi H, Fujita K, Nagatsu T. 1994a. Tumor necrosis factor-alpha (TNF-alpha) increases both in the brain and in the cerebrospinal fluid from parkinsonian patients. Neurosci Lett 165:208–210.

Mogi M, Harada M, Kondo T, Riederer P, Inagaki H, Minami M, Nagatsu T. 1994b. Interleukin-1 beta, interleukin-6, epidermal growth factor and transforming growth factor-alpha are elevated in the brain from parkinsonian patients. Neurosci Lett 180:147–150.

Nagata K, Takei N, Nakajima K, Saito H, Kohsaka S. 1993a. Microglial conditioned medium promotes survival and development of cultured mesencephalic neurons from embryonic rat brain. J Neurosci Res 34:357–363.

Nagata K, Nakajima K, Kohsaka S. 1993b. Plasminogen promotes the development of rat mesencephalic dopaminergic neurons in vitro. Brain Res Dev Brain Res 75:31–37.

Nagatsu I, Kondo Y, Inagaki S, Karasawa N, Kato T, Nagatsu T. 1977. Immunofluorescent studies on tyrosine hydroxylase: application for its axoplasmic transport. Acta Histochem Cytochem 10:494–499.

Nagatsu T, Sawada M. 2005. Inflammatory process in Parkinson's disease: role for cytokines. Curr Pharm Design 11:999–1016.

Nakajima K, Tsuzaki N, Nagata K, Takemoto N, Kohsaka S. 1992. Production and secretion of plasminogen in cultured rat brain microglia. FEBS Lett 308:179–182.

Nakajima K, Honda S, Tohyama Y, Imai Y, Kohsaka S, Kurihara T. 2001. Neurotrophin secretion from cultured microglia. J Neurosci Res 65:322–331.

Rabchevsky AG, Streit WJ. 1997. Grafting of cultured microglial cells into the lesioned spinal cord of adult rats enhances neurite outgrowth. J Neurosci Res 47:34–48.

Sawada M, Kondo N, Suzumura A, Marunouchi T. 1989. Production of tumor necrosis factor-alpha by microglia and astrocytes in culture. Brain Res 491:394–397.

Sawada M, Suzumura A, Yamamoto H, Marunouchi T. 1990. Activation and proliferation of the isolated microglia by colony stimulating factor-1 and possible involvement of protein kinase C. Brain Res 509:119–124.

Sawada M, Suzumura A, Marunouchi T. 1995. Cytokine network in the central nervous system and its roles in growth and differentiation of glial and neuronal cells. Int J Dev Neurosci 13:253–264.

Sawada M, Suzumura A, Hosoya H, Marunouchi T, Nagatsu T. 1999. Interleukin-10 inhibits both production of cytokines and expression of cytokine receptors in microglia. J Neurochem 72:1466–1471.

Sawada M, Imamura K, Nagatsu T. 2006. Role of cytokines in inflammatory process in Parkinson's disease. J Neural Transm Suppl:373–381.

Schmued LC, Hopkins KJ. 2000. Fluoro-Jade B: a high affinity fluorescent marker for the localization of neuronal degeneration. Brain Res 874:123–130.

Sugama S, Yang L, Cho BP, DeGiorgio LA, Lorenzl S, Albers DS, Beal MF, Volpe BT, Joh TH. 2003. Age-related microglial activation in 1-methyl-4-phenyl-1,2,3,6-tetrahydropyridine (MPTP)-induced dopaminergic neurodegeneration in C57BL/6 mice. Brain Res 964:288–294.

Suzuki H, Imai F, Kanno T, Sawada M. 2001. Preservation of neurotrophin expression in microglia that migrate into the gerbil's brain across the blood-brain barrier. Neurosci Lett 312:95–98.

Suzumura A, Sawada M, Yamamoto H, Marunouchi T. 1993. Transforming growth factor-β suppresses activation and proliferation of microglia in vitro. J Immunol 151:2150–2158.

Thery C, Hetier E, Evrard C, Mallat M. 1990. Expression of macrophage colony-stimulating factor gene in the mouse brain during development. J Neurosci Res 26:129–133.

Viel JJ, McManus DQ, Smith SS, Brewer GJ. 2001. Age- and concentration-dependent neuroprotection and toxicity by TNF in cortical neurons from β-amyloid. J Neurosci Res 64:454–465.

Vilhardt F, Plastre O, Sawada M, Suzuki K, Wiznerowicz M, Kiyokawa E, Trono D, Krause KH. 2002. The HIV-1 Nef protein and phagocyte NADPH oxidase activation. J Biol Chem 277:42136–42143.

Wu DC, Jackson-Lewis V, Vila M, Tieu K, Teismann P, Vadseth C, Choi DK, Ischiropoulos H, Przedborski S. 2002. Blockade of microglial activation is neuroprotective in the 1-methyl-4-phenyl-1,2,3,6-tetrahydropyridine mouse model of Parkinson disease. J Neurosci 22:1763–1771.

Wu DC, Teismann P, Tieu K, Vila M, Jackson-Lewis V, Ischiropoulos H, Przedborski S. 2003. NADPH oxidase mediates oxidative stress in the 1-methyl-4-phenyl-1,2,3,6-tetrahydropyridine model of Parkinson's disease. Proc Natl Acad Sci U S A 100:6145–6150.

Neurobiology of Aging 29 (2008) 574–585

Selective loss of nigral dopamine neurons induced by overexpression of truncated human α-synuclein in mice

Masaki Wakamatsu, Aiko Ishii, Shingo Iwata, Junko Sakagami, Yuriko Ukai, Mieko Ono, Daiji Kanbe, Shin-ichi Muramatsu, Kazuto Kobayashi, Takeshi Iwatsubo, Makoto Yoshimoto

Reprinted from NEUROBIOLOGY OF AGING, Vol. 29, No. 4, April 2008

ELSEVIER

Neurobiology of Aging 29 (2008) 574–585

NEUROBIOLOGY OF AGING

www.elsevier.com/locate/neuaging

Selective loss of nigral dopamine neurons induced by overexpression of truncated human α-synuclein in mice☆

Masaki Wakamatsu[a], Aiko Ishii[a], Shingo Iwata[a], Junko Sakagami[a], Yuriko Ukai[a], Mieko Ono[a], Daiji Kanbe[a], Shin-ichi Muramatsu[b], Kazuto Kobayashi[c], Takeshi Iwatsubo[d], Makoto Yoshimoto[a,*]

[a] *Medicinal Research Laboratories, Taisho Pharmaceutical Co., Ltd., Yoshino-cho 1-403, Kita-ku, Saitama-shi, Saitama 331-9530, Japan*
[b] *Division of Neurology, Department of Medicine, Jichi Medical University, Shimotsuke-shi, Tochigi 329-0498, Japan*
[c] *Department of Molecular Genetics, Institute of Biomedical Sciences, Fukushima Medical University School of Medicine, Fukushima-shi, Fukushima 960-1295, Japan*
[d] *Department of Neuropathology and Neuroscience, Graduate School of Pharmaceutical Sciences, University of Tokyo, Bunkyo-ku, Tokyo 113-0033, Japan*

Received 18 July 2006; received in revised form 4 October 2006; accepted 16 November 2006
Available online 14 December 2006

Abstract

Parkinson's disease is characterized by loss of nigral dopaminergic neurons and presence of Lewy bodies, whose major component is α-synuclein. In the present study, we generated transgenic mice termed Syn130m that express truncated human α-synuclein (amino acid residue number: 1–130) in dopaminergic neurons. Notably, dopaminergic neurons were selectively diminished in the substantia nigra pars compacta of Syn130m, while transgenic mice that expressed comparable amount of full-length human α-synuclein did not develop such pathology. Therefore, the truncation of human α-synuclein seems to be primarily responsible for the loss of nigral dopaminergic neurons. The nigral pathology resulted in impairment of axon terminals in the striatum and concomitant decrease in striatal dopamine content. Behaviorally, spontaneous locomotor activities of Syn130m were reduced, but the abnormality was ameliorated by treatment with L-DOPA. The loss of nigral dopaminergic neurons was not progressive and seemed to occur during embryogenesis along with the onset of expression of the transgene. Our results indicate that truncated human α-synuclein is deleterious to the development and/or survival of nigral dopaminergic neurons.

Keywords: Parkinson's disease; Animal model; α-Synuclein; Transgenic mouse; Tyrosine hydroxylase; Dopamine neuron

1. Introduction

Parkinson's disease (PD) is the second most common neurodegenerative disorder clinically characterized by a variety of motor dysfunctions such as bradykinesia, rigidity, resting tremor and postural abnormalities. These symptoms are attributed to the reduction of striatal dopamine (DA) level, which results from selective and progressive degeneration of DAergic neurons in the substantia nigra pars compacta (SNc). Recent studies have demonstrated that point mutations, Ala53Thr (A53T), Ala30Pro and Glu46Lys, in the α-synuclein gene and triplication of a chromosomal region spanning the α-synuclein gene are individually responsible for the onset of autosomal dominant PD in several pedigrees (Kruger et al., 1998; Polymeropoulos et al., 1997; Singleton et al., 2003; Zarranz et al., 2004). In addition, it has been reported that α-synuclein is a major structural component of Lewy bodies (LBs), which are cytoplasmic inclusions and pathological hallmarks of PD (Arawaka et al., 1998; Arima et

Abbreviations: DA, dopamine; H&E, hematoxylin and eosin; LB, Lewy body; PD, Parkinson's disease; SNc, substantia nigra pars compacta; Tg, transgenic; TH, tyrosine hydroxylase; VTA, ventral tegmental area

☆ Kazuto Kobayashi and Takeshi Iwatsubo received grants from Taisho Pharmaceutical Co., Ltd.

* Corresponding author. Tel.: +81 48 669 3095; fax: +81 48 652 7254.
E-mail address: m.yoshimoto@po.rd.taisho.co.jp (M. Yoshimoto).

0197-4580/$ – see front matter © 2006 Elsevier Inc. All rights reserved.
doi:10.1016/j.neurobiolaging.2006.11.017

al., 1998; Baba et al., 1998; Spillantini et al., 1998; Takeda et al., 1998; Wakabayashi et al., 1997). The above background strongly suggests that α-synuclein plays an important role in the pathogenesis of PD.

α-Synuclein is a presynaptic protein composed of 140 amino acid residues and was first discovered as the precursor protein of non-Aβ component of Alzheimer's disease amyloid or NACP (Iwai et al., 1995; Ueda et al., 1993). Accumulating evidence indicates that at least a part of α-synuclein in LBs is truncated from the C-terminus (Baba et al., 1998; Campbell et al., 2001; Liu et al., 2005; Tofaris et al., 2003), and that C-terminal truncation accelerates aggregation of α-synuclein in vitro (Crowther et al., 1998; Du et al., 2003; Murray et al., 2003). In addition, a recent report indicates that the C-terminal truncation of α-synuclein is a normal cellular process (Liu et al., 2005). These data imply that aberrant truncation of α-synuclein has some relevance to the pathogenesis of PD. However, it is not clear at this stage if the processing is actually involved in the development of the disease.

To examine the in vivo function of truncated α-synuclein, we generated transgenic (Tg) mice that express the C-terminally truncated α-synuclein carrying an A53T point mutation under the control of the rat tyrosine hydroxylase (TH) promoter, which enables the transgene to be expressed in DAergic neurons. The truncation was determined to be 10 amino acid residues for the following reasons: (1) Truncation by 10 residues kept the epitope for LB509 (amino acid residue number: 115–122), a monoclonal antibody which discriminates between human α-synuclein and mouse α-synuclein (Jakes et al., 1999). Therefore, expression of the transgene was readily and specifically detected by using LB509. (2) Recombinant α-synuclein with the deletion formed aggregates much faster than full-length α-synuclein in vitro. (3) Ser129, which is mainly phosphorylated in LBs (Fujiwara et al., 2002), was retained in truncated α-synuclein. Thus, the possible involvement of this modification in the phenotype of Tg mice could be investigated.

Remarkably, there was a considerable and selective loss of DAergic neurons in the SNc of the Tg mice. In addition, the Tg mice showed behavioral abnormality which was rectified by the administration of L-DOPA, the most commonly used drug to treat PD. Thus, the Tg mice of the present study developed some of the typical symptoms of PD.

2. Materials and methods

2.1. Construction of TH-α-synuclein transgenes

A DNA fragment containing the 9-kb 5′-flanking region of the rat TH gene was prepared by digesting pTH/-9 kb (Iwawaki et al., 2000) with *Xho*I and *Hin*dIII, and inserted into pBST-N (Kobayashi et al., 1992) to construct pRTH-BstN. A cDNA fragment encoding human α-synuclein was prepared by reverse transcription-polymerase chain reaction (RT-PCR) using human brain RNA as a template, and a point mutation, GCA (Ala53) → ACA (Thr53), was introduced into the gene. A cDNA fragment (1.2 kb) containing the α-synuclein(A53T) gene was inserted into the *Eco*RI site of pRTH-BstN, resulting in a recombinant plasmid, pRTH-Syn140m. Another PCR was carried out to introduce a stop codon just after the 130th residue of human α-synuclein(A53T) by using pRTH-Syn140m as a template and the following oligonucleotides as primers: 5′-ggaattcattagccatggatgtattc and 5′-tagccttaagttactcagaaggcattt. The resultant DNA fragment (417 bp) was similarly inserted into pRTH-BstN to construct pRTH-Syn130m.

2.2. Generation of Tg mice

The recombinant plasmids were digested with *Sal*I, and transgene constructs of 12.2 kb (pRTH-Syn140m) and 11.5 kb (pRTH-Syn130m) were purified (Fig. 1a). The constructs were individually microinjected into the pronuclei of fertilized eggs of B6C3F1 hybrid according to the standard procedure (Hogan et al., 1994). Offspring were screened for the transgene by PCR analysis of DNA extracted from tail biopsies using the following primer set: 5′-gtggctgctgctgagaaaac (P1) and 5′-gtggggctccttcttcattc (P2). Each founder mouse was backcrossed with C57BL/6J mice, and all subsequent studies were performed with N4 or later generations. Tg mice at 8 weeks of age and age-matched non-Tg littermates were analyzed in this study unless otherwise mentioned. All the animal experiments reported here were carried out in accordance with guidelines of the Japanese Association for Laboratory Animal Science.

2.3. Immunoblot analysis

The midbrain and the striatum of adult mice were dissected in consultation with the respective brain maps (Paxinos and Franklin, 2001). The coordinates measured from the interaural line were as follows: from 6.0 to 2.0 mm for the striatum, and from 2.0 to −1.6 mm for the midbrain. The cortex and the hippocampus were removed from the midbrain sections. Cytoplasmic fractions prepared from the brain sections were subjected to immunoblot analysis according to the method described previously (Wakabayashi et al., 1997). The primary antibodies used for the analysis were LB509 (1:750 dilution), a mouse monoclonal antibody that specifically recognizes human α-synuclein (Zymed Laboratories, South San Francisco, CA), NACP5 (1:5000 dilution), a rabbit polyclonal antibody that reacts with both human and mouse α-synuclein and does not crossreact with β-synuclein (Wakabayashi et al., 2000), a rabbit anti-NSE antibody (1:1000 dilution; Polysciences, Warrington, PA) and a rabbit anti-TH antibody (1:400 dilution; Novus Biologicals, Littleton, CO). The intensities of the bands were quantified with ImageMaster 1D Elite (Amersham Biosciences, Tokyo, Japan).

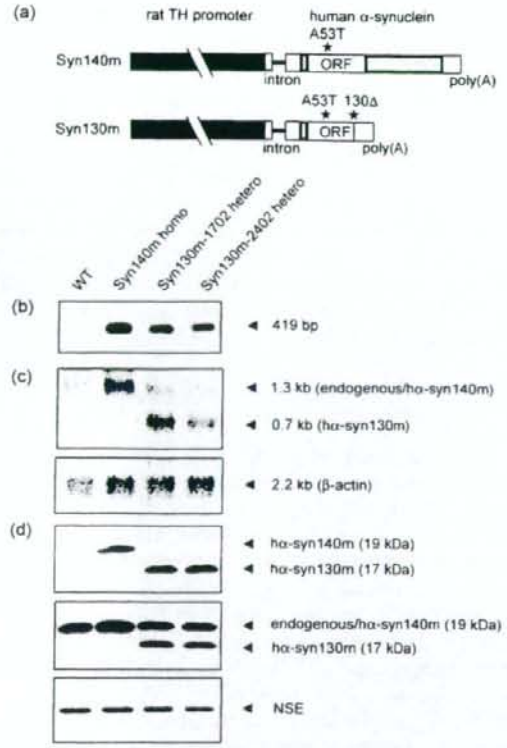

Fig. 1. Expression of the transgenes: (a) Schematic structures of the transgene constructs used to generate Syn140m and Syn130m mice. The constructs contain the rat TH promoter (closed box), the second intron of rabbit β-globin gene, open reading frame (ORF) of the human α-synuclein gene, and an SV40 poly(A) addition signal. Gray boxes indicate 5′- and 3′-untranslated regions of the gene. (b) Southern blot analysis. Genomic DNAs (10 μg) extracted from tail biopsies of Tg mice (heterozygous Syn130m-1702 and Syn130m-2402, and homozygous Syn140m mice) and age-matched non-Tg littermates (WT) were digested with *Eco*RI, electrophoresed, and transferred onto a membrane. The membrane was incubated with a digoxigenin (DIG)-labeled α-synuclein probe prepared by PCR using pRTH-Syn140m as a template and P1 and P2 (see Section 2.2) as primers. (c) Northern blot analysis. Poly(A)$^+$ RNAs (4 μg) extracted from the whole brain were electrophoresed and transferred onto a membrane. The membrane was hybridized with the DIG-labeled α-synuclein probe (upper panel), dehybridized, and reprobed with a DIG-labeled β-actin cDNA (lower panel). (d) Immunoblot analysis. Cytoplasmic proteins (50 μg) prepared from the midbrain were separated through an SDS-polyacrylamide gel and transferred onto a membrane. The membrane was probed with either LB509 (upper panel), NACP5 (middle panel) or anti-NSE antibody (lower panel).

2.4. Immunohistochemical analysis

The dissected brain was embedded in paraffin and 3 μm-thick serial sections were prepared. To prepare 'mirror sections', the cutting side of two adjacent sections were placed face up on a slide glass. The sections were incubated with LB509 (1:2000 dilution), NACP5 (1:600 dilution) or anti-TH antibody (1:400 dilution). Biotin-labeled secondary antibodies (Vector Laboratories, Burlingame, CA) were used at 10 μg/ml. Immunoreactivities were detected with diaminobenzidine, and nuclei were counterstained with hematoxylin. For double immunofluorescence staining, Alexa Fluor 488 goat anti-mouse IgG and Alexa Fluor 568 goat anti-rabbit IgG (Invitrogen, Carlsbad, CA) were used as secondary antibodies at a dilution of 1:1000.

2.5. Quantification of DAergic neurons

Three micrometer-thick serial sections were prepared from the midbrain and stained with anti-TH antibody. The sections were observed at low magnification (4× objective), and the SNc and the ventral tegmental area (VTA) regions were individually outlined according to the brain map (Paxinos and Franklin, 2001). The section with the following anatomical landmark was designated as section #2; that is, a section in which the SNc was divided by the medial terminal nucleus of the accessory optic tract (i.e., the coordinate measured from the interaural line was 0.64 mm). The number of TH-positive cells in sections from #1 to #8 (30 μm intervals) was counted at higher magnification (40× objective) by the fractionator procedure using the StereoInvestigator system (MicroBrightfield, Williston, VT).

2.6. Real-time PCR analysis

Total RNA (1 μg) extracted from the midbrain or the whole embryonic brain was subjected to reverse transcription in the presence of 0.2 μg of oligo(dT)$_{12-18}$. Real-time quantitative PCR was carried out with SYBR Green PCR Master mix (Applied Biosystems, Foster City, CA). Gene-specific primers used for the analysis were as follows: TH, 5′-ttgaaggaacggactggctt and 5′-gaaacacacggaaggccaga; DA transporter (DAT), 5′-ccgtatctgtgaggcatctgt and 5′-aacgccaagggagaagcac; c-ret, 5′-tagccactgaccggcagac and 5′-aatggatgtcccctccacag; glutamic acid decarboxylase 1 (GAD1), 5′-agcatcatggctgctcgttacaag and 5′-attgtcggttccaaagccaagc; glial fibrillary acidic protein (GFAP), 5′-agctcaatgaccgctttgctag and 5′-ctggtagacatcagccagtttg; S26 ribosomal protein (Vincent et al., 1993), 5′-ccccaccacgattcagacc and 5′-acggcctctttacatgggc. A primer set for glyceraldehyde 3-phosphate dehydrogenase (GAPDH) was purchased from Applied Biosystems. The cycle profile consisted of 1 min at 95 °C for denaturation and 1 min at 60 °C for annealing and primer extension. Fluorescence was detected by ABI PRISM 7700 sequence detection systems (Applied Biosystems), and mRNA levels were normalized relative to that of GAPDH.

2.7. Measurement of monoamine contents

Brain sections were homogenized in a buffer containing 0.2 M perchloric acid, 100 μM ethylenediaminetetraacetic acid (EDTA) and 10 μM pargyline. After centrifugation, DA, its metabolites [i.e., homovanillic acid (HVA) and 3,4-dihydroxyphenylacetic acid (DOPAC)] and serotonin in the supernatant were separated thorough EICOMPAK SC-5ODS

(150 mm × 3.0 mm, Eicom, Kyoto, Japan) with a mobile phase consisting of 0.1 M citrate–acetate buffer, pH 3.9, 18% methanol, 190 mg/l sodium octanslufonate and 5 mg/l EDTA (column temperature: 30 °C; flow-rate: 0.5 ml/min), and detected with an electrochemical detector (NANOSPACE SI-1/2005, Shiseido, Tokyo, Japan). External standards were similarly separated after each chromatographic run for identification and quantification of the peaks.

2.8. Behavioral tests

Male Tg mice and age-matched non-Tg littermates were individually housed into an opaque polypropylene cage with ad libitum access to food and water during 12-h light:12-h dark cycle in a sound-proof room. The mice were allowed to acclimatize to the new environment for 15 h before experiment. Spontaneous locomotor activities were recorded with Absystem apparatus (Neuroscience, Tokyo, Japan). L-DOPA (Sigma, St. Louis, MO) was suspended in saline containing 0.1% ascorbic acid. The suspension, which did not contain a DOPA-decarboxylase inhibitor, was subcutaneously administered at a dose of 150 mg/kg, and spontaneous locomotor activities were recorded for 3 h. The concentration of L-DOPA employed in the present study was within the appropriate range especially when a DOPA-decarboxylase inhibitor was not co-administered (Kaur and Starr, 1995; Sotnikova et al., 2005).

2.9. Statistical analysis

The data are presented as mean ± S.E.M. Differences between groups were examined for statistical significance using two-tailed Student's *t*-test (for single comparison), one-way analysis of variance (ANOVA) followed by Dunnett's multiple comparison test or two-way ANOVA when appropriate. A *p*-value less than 0.05 denoted the presence of a statistically significant difference.

3. Results

3.1. Generation of Tg mice

We generated nine Tg lines that expressed human α-synuclein that carried an A53T point mutation and lacked 10 amino acid residues from the C-terminus (hα-syn130m) under the control of the rat TH promoter (i.e., the 9-kb 5′-flanking region of the rat TH gene; Fig. 1a), which drives tissue-specific expression of a reporter gene in transgenic mice (Min et al., 1994). Two independent high expressing lines were selected and named Syn130m-1702 and Syn130m-2402. FISH analysis showed that the insertion sites of the transgene were 8B3 and 12B3 for lines 1702 and 2402, respectively. As a control, we also generated five Tg lines that expressed full-length human α-synuclein(A53T) (hα-syn140m) under the control of the same promoter (Fig. 1a), and the highest expressing line was named Syn140m. Homozygous Syn140m mice were generated so that the expression level of the transgene was comparable to those of heterozygous Syn130m mice. Thus, heterozygous Syn130m and homozygous Syn140m mice were analyzed hereafter unless otherwise mentioned.

Expression of the transgenes in the brain of Syn130m and Syn140m mice was analyzed, and the results are shown in Fig. 1(b–d). The estimated copy numbers of the transgenes per haploid genome were approximately 30 for Syn130m-1702 and 20 for Syn130m-2402 and Syn140m (Fig. 1b). The results of Northern blot analysis were consistent with the copy numbers (Fig. 1c). Immunoblot analysis with LB509 detected single bands of approximately 17 and 19 kDa, which correspond to hα-syn130m and hα-syn140m, respectively (Fig. 1d; upper panel). NACP5 reacted with hα-syn140m as well as mouse α-synuclein migrated at the same position in the gel for Syn140m mice, while the antibody detected two discrete bands corresponding to hα-syn130m (lower band) and mouse α-synuclein (upper band) for Syn130m mice (Fig. 1d; middle panel).

Quantitative immunoblot analysis of the transgene products in the midbrain indicated that the total amounts of α-synuclein (i.e., the transgene product + mouse α-synuclein) in the midbrain of Syn140m, Syn130m-1702 and Syn130m-2402 were 56.8 ± 1.5, 50.5 ± 1.8 and 45.7 ± 1.1 ng per 100 μg of cytoplasmic protein, which were 1.62, 1.44 and 1.31 times, respectively, more abundant than those in age-matched non-Tg littermates. The expression levels of the transgenes in the midbrain did not change significantly by aging; i.e., 103.1 ± 9.3 and 86.8 ± 3.8% at 52 weeks of age compared with 8 weeks of age for Syn140m and Syn130m-1702, respectively. These data indicate that the rat TH promoter is almost constitutively active in the midbrain for at least 52 weeks.

3.2. Immunohistochemical analysis of the brain of Tg mice

We carried out immunostaining of coronal sections through the midbrain of Tg mice with LB509 and an anti-TH antibody. Since basically similar results were obtained with both of the Syn130m lines, representative data for line 1702 are shown. LB509 detected the transgene products in the soma and axons of neurons in the SNc [closed arrowheads in Fig. 2a (Syn130m) and b (Syn140m)] and the VTA [open arrowheads in Fig. 2a (Syn130m) and b (Syn140m)]. On the other hand, no immunoreactivity was observed in the corresponding areas of age-matched non-Tg littermates (Fig. 2c). Examination of 'mirror sections' prepared from the midbrain of Tg mice indicated that the transgene products were localized not only in the cytoplasm, but also in the nuclei (Fig. 2d; closed arrowhead), while TH was localized only in the cytoplasm (Fig. 2e; closed arrowhead). The transgene products were transported to presynaptic termini in the striatum (Fig. 2f) and the nucleus accumbens (data

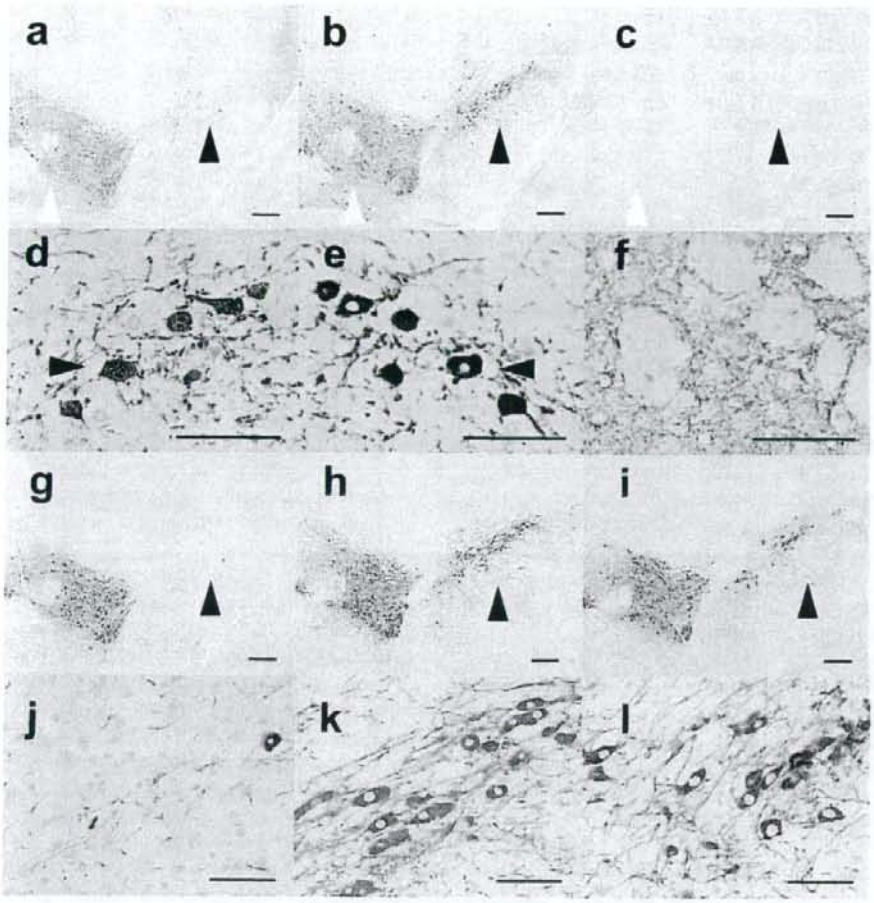

Fig. 2. Immunohistochemical analysis of the brain of Tg mice. (a–c) Coronal sections prepared from the midbrain of Syn130m-1702 (a), Syn140m (b) and an age-matched non-Tg littermate (c), were stained with LB509. Open and closed arrowheads indicate the VTA and SNc, respectively. (d and e) Mirror sections prepared from the SNc region of Syn140m mice were stained with either LB509 (d) or anti-TH antibody (e). Closed arrowheads indicate the same neuron. (f) A section prepared from the striatum of Syn140m mice was stained with LB509. Coordinate measured from the interaural line was 4.8 mm. (g–l) The midbrain of Syn130m-1702 (g and j), Syn140m mice (h and k) and age-matched non-Tg littermates (i and l) were stained with anti-TH antibody. The midbrain was observed at lower magnification (g–i), and the SNc region was observed at higher magnification (j–l). Closed arrowheads in g–i indicate the SNc. Scale bar: 50 μm (a–c and g–i) or 200 μm (d–f and j–l).

not shown), which receive projections from the SNc and the VTA, respectively. The expression profiles of the transgenes were indistinguishable to each other between Syn140m and Syn130m mice, indicating that the C-terminal truncation by at least 10 amino acid residues did not affect the localization of human α-synuclein.

Notably, LB509-immunoreacitvity in the SNc of Syn130m mice (Fig. 2a; closed arrowhead) was weaker than that of Syn140m mice (Fig. 2b; closed arrowhead). Moreover, the TH-immunoreactivity was reduced in the SNc of Syn130m mice (Fig. 2g; closed arrowhead) compared with Syn140m mice (Fig. 2h; closed arrowhead) or non-Tg littermates (Fig. 2i; closed arrowhead). Examination of this region at higher magnification demonstrated this reduction more clearly [Fig. 2j (Syn130m) versus k (Syn140m) and l (non-Tg littermates)]. These data raised the possibility that DAergic neurons were diminished in the SNc of Syn130m mice. In order to test this hypothesis, we carried out a series of experiments. First, locations of TH-positive neurons in sections prepared from the midbrain were spotted on the brain map. This analysis clearly demonstrated a decrease in the number of TH-positive neurons in the SNc of Syn130m mice (Fig. 3a; closed circles) compared with non-Tg littermates (Fig. 3b; closed circles). In particular, the TH-positive neurons were markedly diminished in the lateral part of the SNc in Syn130m mice (Fig. 3a; top and middle arrowheads). On the other hand, the nigral TH-positive neurons clustered on the border of the VTA seemed to be

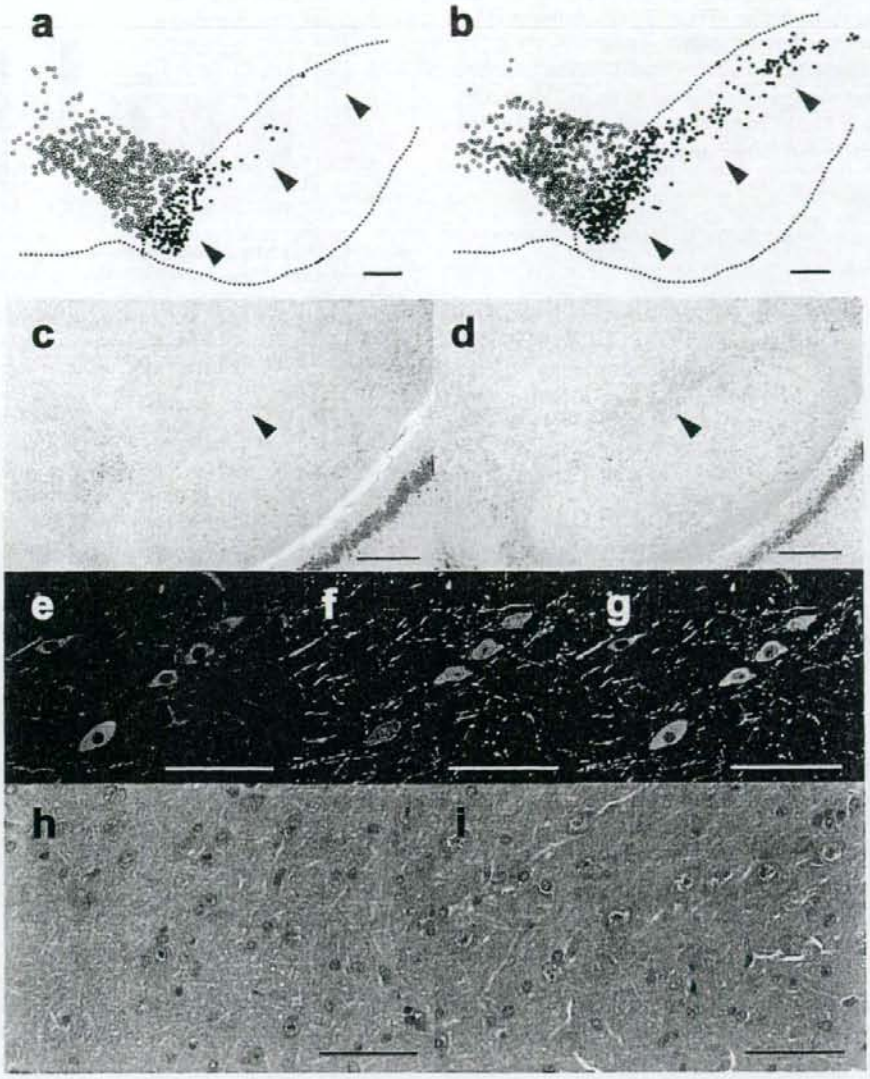

Fig. 3. Neuropathology in the SNc of Syn130m mice. (a and b) Serial sections prepared from the midbrain were stained with anti-TH antibody, and eight sections were selected as described in Materials and methods. The locations of TH-positive neurons in sections #1 to #4 for Syn130m-1702 (a) and an age-matched non-Tg littermate (b) are spotted on the brain map. DAergic neurons in the SNc and the VTA are indicated by closed and open circles, respectively. (c and d) Nissl staining was applied to coronal sections (50 μm-thick) through the midbrain of Syn130m-1702 (c) and an age-matched non-Tg littermate (d). Closed arrowheads indicate the SNc region. (e–g) A coronal section through the midbrain of Syn130m-1702 was stained with anti-TH antibody + Alexa Fluor 568 goat anti-rabbit IgG (e) and LB509 + Alexa Fluor 488 goat anti-mouse IgG (f). Images for TH (red; e) and human α-synuclein (green; f) were merged (g). (h and i) H&E staining was applied to coronal sections through the SNc region of Syn130m-1702 (h) and an age-matched non-Tg littermate (i). Scale bar 200 μm (a–d) or 50 μm (e–i).

less affected (Fig. 3a; bottom arrowhead) than those in the lateral part. In marked contrast to the SNc, TH-positive neurons in the VTA were relatively spared even in Syn130m mice [Fig. 3a (Syn130m) versus b (non-Tg littermates); open circles]. Furthermore, Nissl staining revealed considerable loss of neuronal cell bodies in the SNc region of Syn130m mice (Fig. 3c; closed arrowhead) compared with the control mice (Fig. 3d; closed arrowhead). Third, a section through the SNc region of Syn130m mice was subjected to double immunofluorescence staining with LB509 and anti-TH antibody. Merged images of TH (Fig. 3e) and LB509 (Fig. 3f) showed that most of the LB509-positive cells were concomitantly TH-positive (Fig. 3g), though reduced expression of TH in LB509-positive neurons would have resulted in

robust increase in LB509 (+)/TH (−) cells. Finally, H&E staining showed the loss of neurons in the SNc [Fig. 3h (Syn130m) versus i (non-Tg littermates)]. Taken together, these data strongly suggest that the reduction in TH-positive cells in the SNc of Syn130m mice was primarily due to actual loss of DAergic neurons rather than reduced expression of TH.

3.3. Quantification of the loss of nigral DAergic neurons in the Tg mice

Quantification of mesencephalic DAergic neurons in Syn130m mice revealed that approximately 45 and 19% of DAergic neurons were significantly lost in the SNc of Syn130m-1702 (Fig. 4a, SNc; closed bar) and Syn130m-2402 (Fig. 4a, SNc; hatched bar), respectively, compared with non-Tg littermates (Fig. 4a, SNc; open bar) at 8 weeks of age. On the other hand, no apparent loss of nigral DAergic neurons was noted in Syn140m mice at the same age (Fig. 4a, SNc; gray bar). In contrast to the SNc, no such loss was observed in the VTA of Syn130m (Fig. 4a, VTA; closed and hatched bars) and Syn140m mice (Fig. 4a, VTA; gray bar) compared with non-Tg littermates (Fig. 4a, VTA; open bar), indicating a selective neuronal loss in the SNc of Syn130m mice. Interestingly, the loss of nigral DAergic neurons in Syn130m mice was not progressive and was stable

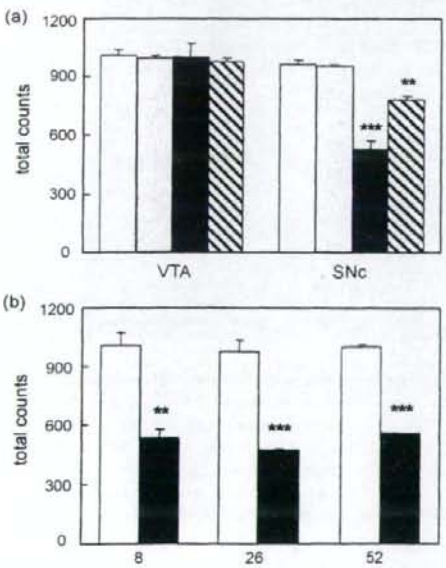

Fig. 4. Quantification of mesencephalic DAergic neurons. The number of TH-positive neurons in the designated area of the midbrain was quantified as described in Section 2.5. (a) The numbers of TH-positive neurons in the VTA and the SNc are individually shown for non-Tg littermates (open bars), Syn140m mice (gray bars), Syn130m-1702 (closed bars) and Syn130m-2402 (hatched bars). (b) The numbers of TH-positive neurons in the SNc of Syn130m-1702 (closed bars) and non-Tg littermates (open bars) were quantified at 8, 26 and 52 weeks of age. $^{**}p<0.01$; $^{***}p<0.001$ ($n=3$).

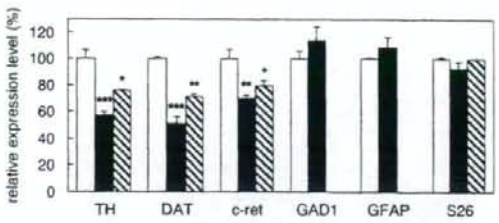

Fig. 5. Real-time PCR analysis of the loss of DAergic neurons. Total RNAs were extracted from the midbrain of Syn130m-1702 (closed bars), Syn130m-2402 (hatched bars) and non-Tg littermates (open bars). The expression levels of TH, DAT, c-ret, GAD1, GFAP and S26 were quantified by real-time PCR analysis. The data were normalized to that for GAPDH. $^{*}p<0.05$; $^{**}p<0.01$; $^{***}p<0.001$ ($n=3$).

up to 52 weeks of age (Fig. 4b). These findings were confirmed by several other methods. Quantitative immunoblot analysis showed that the relative densities of TH in the midbrain of Syn130m-1702 and Syn130m-2402 decreased to 60.2 ± 3.3 and $71.3 \pm 3.8\%$, respectively, relative to those of age-matched non-Tg littermates, while no significant decrease was observed in Syn140m mice. Furthermore, real-time PCR analysis indicated that the expression levels of TH, DAT and c-ret, which are specifically expressed in DAergic neurons, were significantly diminished in the midbrain of Syn130m-1702 (Fig. 5; closed bars) and Syn130m-2402 (Fig. 5; hatched bars) compared with age-matched non-Tg littermates (Fig. 5; open bars). On the other hand, expressions of GAD1 and GFAP, which are predominantly expressed in GABAergic neurons and astrocytes, respectively, were not affected at all in Syn130m mice (Fig. 5). Collectively, these data support the notion that a proportion of DAergic neurons are lost in the SNc of Syn130m mice.

3.4. Behavioral abnormalities of the Tg mice

The data in Figs. 4 and 5 indicate that the loss of nigral DAergic neurons in Syn130m mice was severe in line 1702 than in line 2402. Therefore, the former line was extensively analyzed hereafter. In accordance with the selective loss of nigral DAergic neurons, TH-positive neurites were markedly impaired in the striatum of Syn130m mice (Fig. 6a). On the other hand, no overt abnormalities were observed in the nucleus accumbens which receive projections from the VTA (data not shown). As a result, striatal TH was decreased to $38.1 \pm 3.2\%$ of the control at 8 weeks of age (Fig. 6b; TH). Consequently, striatal contents of DA and HVA, one of the major metabolites of DA, were significantly reduced to 48.8 ± 2.2 and $51.9 \pm 1.6\%$, respectively, relative to those of non-Tg littermates of the same age (Fig. 6b; DA and HVA). The amount of DOPAC, another metabolite of DA, in the striatum was also decreased to a similar extent (data not shown). On the other hand, there was no significant difference in the serotonin content between Syn130m mice and non-Tg littermates (Fig. 6b; serotonin). The amounts of TH and DA in the striatum did not show an age-dependent decrease but

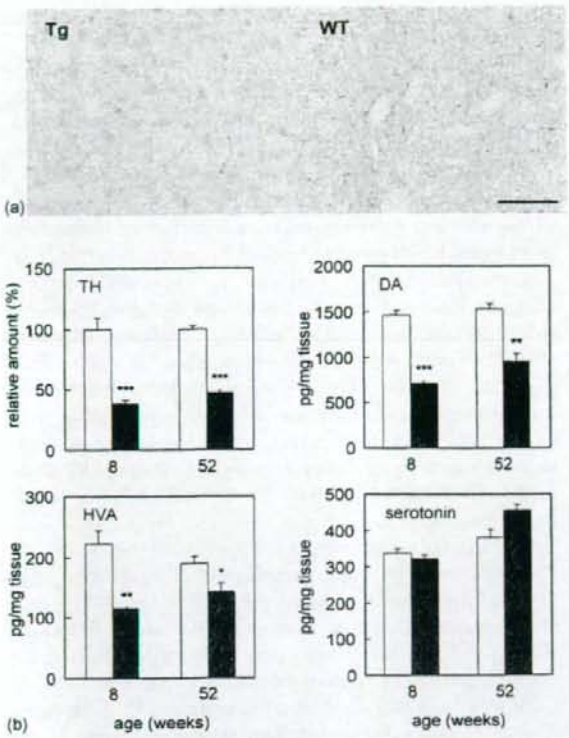

Fig. 6. Neuropathology in the striatum. (a) Coronal sections of the midbrain of Syn130m-1702 (Tg) and an age-matched non-Tg littermate (WT) were stained with anti-TH antibody. Coordinate measured from the interaural line was 2.9 mm. Scale bar: 200 μm. (b) The amounts of TH, DA, HVA and serotonin in the striatum of Syn130m-1702 (closed bars) and age-matched non-Tg littermates (open bars) were measured at 8 and 52 weeks of age. $^{*}p<0.05$; $^{**}p<0.01$; $^{***}p<0.001$ ($n=4$).

plateaued to a similar extent up to 52 weeks of age (Fig. 6b; TH and DA).

The striatal impairments in Syn130m mice prompted us to conduct a battery of motor function tests (e.g. rotarod test, pole test, traction test and catalepsy test). However, no motor deficits were detected by these tests. Notably, both diurnal and nocturnal spontaneous locomotor activities of Syn130m mice were markedly reduced compared with the control (Fig. 7a), though the rectal temperature was not significantly different. It is known that the loss of striatal dopamine causes behavioral deficits, which improve with L-DOPA, the precursor of DA and the most commonly used drug for PD (Tillerson et al., 2002). Therefore, we examined the effect of L-DOPA on the behavioral abnormalities of Syn130m mice. The Tg mice showed significant recovery in locomotor activity following a single subcutaneous injection of L-DOPA (150 mg/kg), whereas the drug at this concentration did not affect the behavior of non-Tg littermates (Fig. 7b). These data suggest that the decrease in the spontaneous locomotor activities of Syn130m mice was related to the striatal DA content.

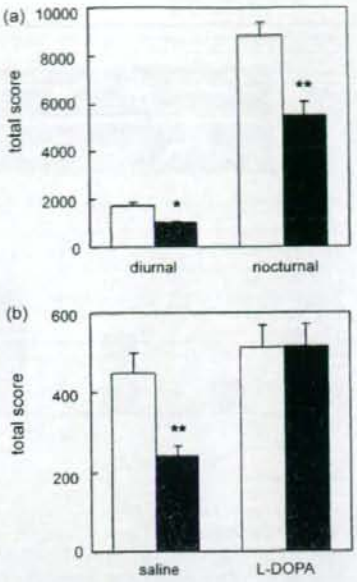

Fig. 7. Effect of L-DOPA on the behavioral abnormalities of Tg mice. (a) Spontaneous locomotor activities of Syn130m-1702 (closed bars) and age-matched non-Tg littermates (open bars) in the light (diurnal) and dark (nocturnal) periods are individually shown. (b) Suspension of L-DOPA (150 mg/kg) was injected subcutaneously in Syn130m-1702 (closed bars) and age-matched non-Tg littermates (open bars) during light period. Spontaneous locomotor activities were measured for 3 h (from 0.5 to 3.5 h after administration). $^{*}p<0.05$; $^{**}p<0.01$ [$n=11$ (a); $n=17$ (b)].

3.5. Loss of nigral DAergic neurons during embryogenesis

In an attempt to elucidate the mechanism of the selective neuronal loss in Syn130m mice, we tried to generate homozygotes of line 1702 expecting much severer phenotype. Genotyping of the embryos revealed that intercross of heterozygotes produced offspring of all three different genotypes according to Mendel's laws, indicating that homozygotes are not embryonic lethal. However, none of the weaned pups was homozygous. We then delivered the offspring by Caesarean section on days 19 post-coitus, and found that homozygotes had relatively higher incidence of apneas after delivery (10/16) compared with heterozygotes (6/28) and non-Tg littermates (2/14). In addition, none of the homozygous neonates survived beyond postnatal day 1. Genotyping and quantitative immunoblot analysis of the neonates indicated that the expression level of hα-syn130m was almost proportional to the gene dosage, while the relative amount of TH was markedly decreased in inverse proportion to the gene dosage (supplemental data). Taken together, these results unequivocally indicate that the loss of DAergic neurons correlate strongly with the expression level of hα-syn130m.

The data described above suggest that the neuronal loss takes place during embryogenesis. To address this issue, we

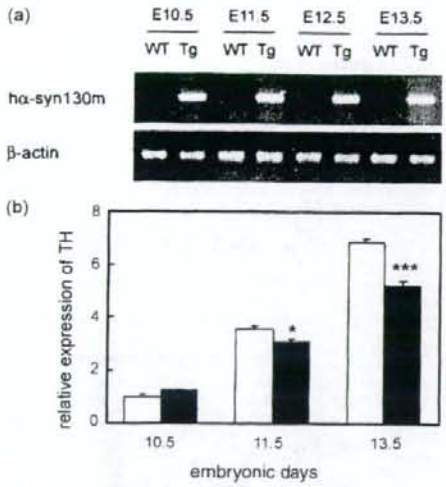

Fig. 8. Analysis of embryonic brain. Total RNAs were extracted from the whole embryonic brain of Syn130m-1702 [Tg (a) and closed bars (b)] and non-Tg littermates [WT (a) and open bars (b)] at E10.5, E11.5, E12.5 and E13.5. (a) Expression of the transgene was analyzed by RT-PCR. (b) Expression of TH was quantified by real-time PCR analysis. The data were normalized to that for GAPDH. $*p<0.05$; $***p<0.001$ ($n=4$–6).

analyzed the embryonic brain prepared at various stages of gestation. RT-PCR analysis revealed that the transgene was turned on even at 10.5 days of gestation (E10.5; Fig. 8a). Notably, the expression level of TH was significantly lower in Syn130m mice after E11.5 than in non-Tg littermates (Fig. 8b). However, the number of TUNEL-positive and anti-activated caspase 3 antibody-positive cells in the embryonic brain of Syn130m mice were not significantly different from the control (data not shown). These data strongly suggest that overexpression of hα-syn130m is deleterious to development and/or survival of nigral DAergic neurons during embryogenesis.

4. Discussion

Several groups had already generated Tg mice that express full-length α-synuclein under the control of various promoters (Giasson et al., 2002; Kahle et al., 2000; Lee et al., 2002; Masliah et al., 2000; Matsuoka et al., 2001; Neumann et al., 2002; Richfield et al., 2002; van der Putten et al., 2000). In the present study, we generated Tg mice (Syn130m mice) that express C-terminally truncated human α-synuclein (hα-syn130m) under the control of the rat TH promoter so that the transgene is expressed in mesencephalic DAergic neurons (Fig. 2a). Remarkably, nigral TH-positive neurons (A9 cells) were selectively and constitutively reduced in substantial numbers in Syn130m mice (Figs. 2–4). In marked contrast to A9 cells, DAergic neurons in the VTA (A10 cells) were relatively spared (Figs. 3a and 4a). We concluded that this reduction was due to actual loss of A9 cells rather than reduced expression of TH in these cells based on the data of Nissl-staining (Fig. 3c and d), double immunofluorescence staining (Fig. 3e–g), H&E staining (Fig. 3h and i) and real-time PCR analysis (Fig. 5). Though hα-syn130m was also expressed in catecholamine producing cells in several other tissues, such as olfactory bulb, the locus ceruleus and the adrenal medulla, no overt loss of the cells was observed in these loci (data not shown). Therefore, the loss of DAergic neurons seemed to occur specifically in the SNc. The loss of A9 cells was accompanied by a reduction of nigral TH, impairment of TH-positive neurites in the striatum (Fig. 6a) and subsequent decrease in the amounts of striatal TH and DA (Fig. 6b). Examination of the behavioral parameters demonstrated the impairment of spontaneous locomotor activities (Fig. 7a). Since L-DOPA treatment significantly ameliorated the locomotor deficit (Fig. 7b), we postulate that this behavioral abnormality was due to low striatal DA content (Fig. 6b). Other motor functions thus far examined were not impaired in Syn130m mice, probably because the residual DA level in the striatum was still above the threshold to cause other motor dysfunctions.

We carefully and extensively analyzed the brain of Syn130m mice for other pathological abnormalities, and obtained the following results: (1) H&E staining (Fig. 3h) and immunostaining with an anti-GFAP antibody (data not shown) did not detect any sign of gliosis, which generally accompanies neurodegeneration (Vila et al., 2001). Lack of gliosis was confirmed by real-time PCR analysis (Fig. 5). Moreover, immunostaining against Iba1 showed lack of microgliosis (data not shown). These results imply that inflammatory process was not involved in the neuronal loss in Syn130m mice. Given that hα-syn130m is deleterious to the development and/or survival of A9 cells (see below), lack of gliosis is not surprising. (2) It is known that α-synuclein is phosphorylated mainly at Ser129 in LBs (Fujiwara et al., 2002) suggesting that the modification is involved in the pathogenesis of PD (Chen and Feany, 2005). However, DAergic neurons were only faintly immunoreactive to an antibody which specifically reacts to α-synuclein phosphorylated at Ser129 (data not shown) (Fujiwara et al., 2002). This is probably because hα-syn130m lacks a part of the consensus recognition sequence for casein kinases or G-protein coupled receptor kinases, which were reported to be responsible for the phosphorylation at Ser129 (Okochi et al., 2000; Pronin et al., 2000). Therefore, Ser129 might not have been phosphorylated effectively. (3) It has been reported that C-terminally truncated α-synuclein forms aggregates much faster than the full-length protein in vitro (Crowther et al., 1998; Du et al., 2003; Murray et al., 2003). Though this is also the case with hα-syn130m (Yoshimoto et al., unpublished observations), LB-like structures were not detected in the brain of Syn130m mice by H&E staining (Fig. 3h) or immunostaining with anti-ubiquitin antibodies (data not shown). Moreover, in our hand immunoblot analysis did not detect aggregated α-synuclein in the brain (data not shown). Collectively, it seems that neuronal loss in Syn130m mice took place in the absence of LB formation. These data may be consistent with the finding

that α-synuclein inclusion bodies are not toxic to the neurons (Chen and Feany, 2005).

The data of the present study strongly suggest that overexpression of hα-syn130m is deleterious to normal development and/or survival of A9 cells during embryogenesis (Fig. 8b). The mechanism of the selective toxicity of hα-syn130m remains unclear. The possibility that the phenotype of Syn130m mice was caused by insertional mutagenesis was excluded since the integration sites of the transgene were different from each other for two independent Tg lines which showed similar phenotype (8B3 and 12B3 for lines 1702 and 2402, respectively). It seems that the expression level of the transgene per se is an important factor for the neuronal loss, because loss of A9 cells seemed to be dependent on the expression level of hα-syn130m (Figs. 4a and 5 and supplemental data). In addition, other Tg lines that expressed hα-syn130m at lower level did not develop similar phenotype. Nevertheless, it is likely that truncation of human α-synuclein(A53T) is primarily responsible for the selective loss of A9 cells since homozygous Syn140m mice, in which comparable amount of hα-syn140m was expressed in the midbrain, did not develop such a phenotype at 8 weeks (Figs. 2h and k and 4a) or even at 18 months of age (data not shown). Therefore, it may be conceivable that truncated human α-synuclein gains toxic functions and exerts deleterious effects to A9 cells in a dominant fashion, though the possibility that the truncated protein fails to protect A9 progenitor cells from various insults such as oxidative damage (Albani et al., 2004; Kanda et al., 2000; Liu et al., 2005) cannot be completely ruled out.

Our data suggest that a truncation by only 10 amino acid residues from the C-terminus would be sufficient to produce toxic effects on A9 cells, though several C-terminally truncated species of α-synuclein accumulate in the brain of PD patients (Campbell et al., 2001; Li et al., 2005; Liu et al., 2005; Tofaris et al., 2003). It may be noteworthy that not only A10 cells but also A9 cells clustering on the border of the VTA seem to be relatively less susceptible to the "toxicity" of hα-syn130m (Fig. 3a). These data, together with the fact that the loss of A9 cells was not progressive (Fig. 4b), imply the existence of subpopulations of DAergic neurons within A9 cell groups in terms of susceptibility to hα-syn130m.

Recently, Tofaris et al. (2006) reported a Tg line that express C-terminally truncated human α-synuclein (amino acid residue number: 1–120) under the control of the TH promoter. The major difference between their Tg mice and Syn130m mice is that the former express wild type human α-synuclein(1–120) and lack endogenous α-synuclein, while the latter express both mutant human α-synuclein(1-130) and intact endogenous α-synuclein. Despite the difference in the genetic background and the length of the truncation, striatal DA level was almost constitutively reduced in both of the Tg lines. Therefore, our results complement the notion that C-terminally truncated α-synuclein affects the development of DAergic system. The other reported phenotypes were not observed in our Tg mice (i.e., pathological inclusions and microgliosis). It is currently unclear if these differences are solely derived from the difference in the length of the truncation.

In conclusion, we generated Tg mice that recapitulate some of typical features of PD (i.e., selective loss of nigral DAergic neurons, subsequent decrease in striatal DA content and behavioral abnormalities that can be rectified with L-DOPA). Since DAergic neurons are affected during embryogenesis and the neuronal loss does not progress after birth, these Tg mice have limitations to use as an animal model of PD. However, these Tg mice are useful to investigate the toxicity of α-synuclein to nigral DAergic neurons in vivo. In addition, the early onset of the symptoms is advantageous to explore therapeutic possibilities for PD.

Conflict of interest

Masaki Wakamatsu, Aiko Ishii, Shingo Iwata, Junko Sakagami, Yuriko Ukai, Mieko Ono, Daiji Kanbe and Makoto Yoshimoto are the employees of Taisho Pharmaceutical Co., Ltd. Shin-ichi Muramatsu has no conflicts of interest.

Disclosure

The data in this manuscript have not been previously published, have not been submitted elsewhere and will not be submitted elsewhere while under consideration at Neurobiology of Aging. All the animal experiments reported in this manuscript were carried out in accordance with guidelines of the Japanese Association for Laboratory Animal Science. All authors have reviewed the contents of this manuscript and validated the accuracy of the data.

Acknowledgments

We thank Drs. Hitoshi Takahashi and Akiyoshi Kakita at Brain Disease Research Center, Niigata University for their helpful suggestions during the preparation of this manuscript. We are also grateful to Ms. Keiko Chiba for the technical assistance in the preparation of the transgene constructs. This study was financially supported by Taisho Pharmaceutical Co., Ltd.

Appendix A. Supplementary data

Supplementary data associated with this article can be found, in the online version, at doi:10.1016/j.neurobiolaging.2006.11.017.

References

Albani, D., Peverelli, E., Rametta, R., Batelli, S., Veschini, L., Negro, A., Forloni, G., 2004. Protective effect of TAT-delivered alpha-synuclein:

relevance of the C-terminal domain and involvement of HSP70. Faseb J. 18, 1713–1715.

Arawaka, S., Saito, Y., Murayama, S., Mori, H., 1998. Lewy body in neurodegeneration with brain iron accumulation type 1 is immunoreactive for alpha-synuclein. Neurology 51 (3), 887–889.

Arima, K., Ueda, K., Sunohara, N., Hirai, S., Izumiyama, Y., Tonozuka-Uehara, H., Kawai, M., 1998. Immunoelectron-microscopic demonstration of NACP/alpha-synuclein-epitopes on the filamentous component of Lewy bodies in Parkinson's disease and in dementia with Lewy bodies. Brain Res. 808 (1), 93–100.

Baba, M., Nakajo, S., Tu, P.H., Tomita, T., Nakaya, K., Lee, V.M., Trojanowski, J.Q., Iwatsubo, T., 1998. Aggregation of alpha-synuclein in Lewy bodies of sporadic Parkinson's disease and dementia with Lewy bodies. Am. J. Pathol. 152 (4), 879–884.

Campbell, B.C., McLean, C.A., Culvenor, J.G., Gai, W.P., Blumbergs, P.C., Jakala, P., Beyreuther, K., Masters, C.L., Li, Q.X., 2001. The solubility of alpha-synuclein in multiple system atrophy differs from that of dementia with Lewy bodies and Parkinson's disease. J. Neurochem. 76 (1), 87–96.

Chen, L., Feany, M.B., 2005. Alpha-synuclein phosphorylation controls neurotoxicity and inclusion formation in a Drosophila model of Parkinson disease. Nat. Neurosci. 8 (5), 657–663.

Crowther, R.A., Jakes, R., Spillantini, M.G., Goedert, M., 1998. Synthetic filaments assembled from C-terminally truncated alpha-synuclein. FEBS Lett. 436 (3), 309–312.

Du, H.N., Tang, L., Luo, X.Y., Li, H.T., Hu, J., Zhou, J.W., Hu, H.Y., 2003. A peptide motif consisting of glycine, alanine, and valine is required for the fibrillization and cytotoxicity of human alpha-synuclein. Biochemistry 42 (29), 8870–8878.

Fujiwara, H., Hasegawa, M., Dohmae, N., Kawashima, A., Masliah, E., Goldberg, M.S., Shen, J., Takio, K., Iwatsubo, T., 2002. alpha-Synuclein is phosphorylated in synucleinopathy lesions. Nat. Cell. Biol. 4 (2), 160–164.

Giasson, B.I., Duda, J.E., Quinn, S.M., Zhang, B., Trojanowski, J.Q., Lee, V.M., 2002. Neuronal alpha-synucleinopathy with severe movement disorder in mice expressing A53T human alpha-synuclein. Neuron 34 (4), 521–533.

Hogan, B., Beddington, R., Costantini, F., Lacy, E., 1994. Manipulating the Mouse Embryo, Second ed. Cold Spring Harbor Laboratory Press, Plainview.

Iwai, A., Masliah, E., Yoshimoto, M., Ge, N., Flanagan, L., de Silva, H.A., Kittel, A., Saitoh, T., 1995. The precursor protein of non-A beta component of Alzheimer's disease amyloid is a presynaptic protein of the central nervous system. Neuron 14 (2), 467–475.

Iwawaki, T., Kohno, K., Kobayashi, K., 2000. Identification of a potential nurr1 response element that activates the tyrosine hydroxylase gene promoter in cultured cells. Biochem. Biophys. Res. Commun. 274 (3), 590–595.

Jakes, R., Crowther, R.A., Lee, V.M., Trojanowski, J.Q., Iwatsubo, T., Goedert, M., 1999. Epitope mapping of LB509, a monoclonal antibody directed against human alpha-synuclein. Neurosci. Lett. 269 (1), 13–16.

Kahle, P.J., Neumann, M., Ozmen, L., Muller, V., Jacobsen, H., Schindzielorz, A., Okochi, M., Leimer, U., van Der Putten, H., Probst, A., Kremmer, E., Kretzschmar, H.A., Haass, C., 2000. Subcellular localization of wild-type and Parkinson's disease-associated mutant alpha-synuclein in human and transgenic mouse brain. J. Neurosci. 20 (17), 6365–6373.

Kanda, S., Bishop, J.F., Eglitis, M.A., Yang, Y., Mouradian, M.M., 2000. Enhanced vulnerability to oxidative stress by alpha-synuclein mutations and C-terminal truncation. Neuroscience 97 (2), 279–284.

Kaur, S., Starr, M.S., 1995. Antiparkinsonian action of dextromethorphan in the reserpine-treated mouse. Eur. J. Pharmacol. 280 (2), 159–166.

Kobayashi, K., Sasaoka, T., Morita, S., Nagatsu, I., Iguchi, A., Kurosawa, Y., Fujita, K., Nomura, T., Kimura, M., Katsuki, M., Nagatsu, T., 1992. Genetic alteration of catecholamine specificity in transgenic mice. Proc. Natl. Acad. Sci. U.S.A. 89 (5), 1631–1635.

Kruger, R., Kuhn, W., Muller, T., Woitalla, D., Graeber, M., Kosel, S., Przuntek, H., Epplen, J.T., Schols, L., Riess, O., 1998. Ala30Pro mutation in the gene encoding alpha-synuclein in Parkinson's disease. Nat. Genet. 18 (2), 106–108.

Lee, M.K., Stirling, W., Xu, Y., Xu, X., Qui, D., Mandir, A.S., Dawson, T.M., Copeland, N.G., Jenkins, N.A., Price, D.L., 2002. Human alpha-synuclein-harboring familial Parkinson's disease-linked Ala-53 → Thr mutation causes neurodegenerative disease with alpha-synuclein aggregation in transgenic mice. Proc. Natl. Acad. Sci. U.S.A. 99 (13), 8968–8973.

Li, W., West, N., Colla, E., Pletnikova, O., Troncoso, J.C., Marsh, L., Dawson, T.M., Jakala, P., Hartmann, T., Price, D.L., Lee, M.K., 2005. Aggregation promoting C-terminal truncation of alpha-synuclein is a normal cellular process and is enhanced by the familial Parkinson's disease-linked mutations. Proc. Natl. Acad. Sci. U.S.A. 102 (6), 2162–2167.

Liu, C.W., Giasson, B.I., Lewis, K.A., Lee, V.M., Demartino, G.N., Thomas, P.J., 2005. A precipitating role for truncated alpha-synuclein and the proteasome in alpha-synuclein aggregation: implications for pathogenesis of Parkinson disease. J. Biol. Chem. 280 (24), 22670–22678.

Masliah, E., Rockenstein, E., Veinbergs, I., Mallory, M., Hashimoto, M., Takeda, A., Sagara, Y., Sisk, A., Mucke, L., 2000. Dopaminergic loss and inclusion body formation in alpha-synuclein mice: implications for neurodegenerative disorders. Science 287 (5456), 1265–1269.

Matsuoka, Y., Vila, M., Lincoln, S., McCormack, A., Picciano, M., LaFrancois, J., Yu, X., Dickson, D., Langston, W.J., McGowan, E., Farrer, M., Hardy, J., Duff, K., Przedborski, S., Di Monte, D.A., 2001. Lack of nigral pathology in transgenic mice expressing human alpha-synuclein driven by the tyrosine hydroxylase promoter. Neurobiol. Dis. 8 (3), 535–539.

Min, N., Joh, T.H., Kim, K.S., Peng, C., Son, J.H., 1994. 5′ upstream DNA sequence of the rat tyrosine hydroxylase gene directs high-level and tissue-specific expression to catecholaminergic neurons in the central nervous system of transgenic mice. Brain Res. Mol. Brain Res. 27 (2), 281–289.

Murray, I.V., Giasson, B.I., Quinn, S.M., Koppaka, V., Axelsen, P.H., Ischiropoulos, H., Trojanowski, J.Q., Lee, V.M., 2003. Role of alpha-synuclein carboxy-terminus on fibril formation in vitro. Biochemistry 42 (28), 8530–8540.

Neumann, M., Kahle, P.J., Giasson, B.I., Ozmen, L., Borroni, E., Spooren, W., Muller, V., Odoy, S., Fujiwara, H., Hasegawa, M., Iwatsubo, T., Trojanowski, J.Q., Kretzschmar, H.A., Haass, C., 2002. Misfolded proteinase K-resistant hyperphosphorylated alpha-synuclein in aged transgenic mice with locomotor deterioration and in human alpha-synucleinopathies. J. Clin. Invest. 110 (10), 1429–1439.

Okochi, M., Walter, J., Koyama, A., Nakajo, S., Baba, M., Iwatsubo, T., Meijer, L., Kahle, P.J., Haass, C., 2000. Constitutive phosphorylation of the Parkinson's disease associated alpha-synuclein. J. Biol. Chem. 275 (1), 390–397.

Paxinos, G., Franklin, K.B.J., 2001. The Mouse Brain in Stereotaxic Coordinates, Second ed. Academic Press, San Diego.

Polymeropoulos, M.H., Lavedan, C., Leroy, E., Ide, S.E., Dehejia, A., Dutra, A., Pike, B., Root, H., Rubenstein, J., Boyer, R., Stenroos, E.S., Chandrasekharappa, S., Athanassiadou, A., Papapetropoulos, T., Johnson, W.G., Lazzarini, A.M., Duvoisin, R.C., Di Iorio, G., Golbe, L.I., Nussbaum, R.L., 1997. Mutation in the alpha-synuclein gene identified in families with Parkinson's disease. Science 276 (5321), 2045–2047.

Pronin, A.N., Morris, A.J., Surguchov, A., Benovic, J.L., 2000. Synucleins are a novel class of substrates for G protein-coupled receptor kinases. J. Biol. Chem. 275 (34), 26515–26522.

Richfield, E.K., Thiruchelvam, M.J., Cory-Slechta, D.A., Wuertzer, C., Gainetdinov, R.R., Caron, M.G., Di Monte, D.A., Federoff, H.J., 2002. Behavioral and neurochemical effects of wild-type and mutated human alpha-synuclein in transgenic mice. Exp. Neurol. 175 (1), 35–48.

Singleton, A.B., Farrer, M., Johnson, J., Singleton, A., Hague, S., Kachergus, J., Hulihan, M., Peuralinna, T., Dutra, A., Nussbaum, R., Lincoln, S., Crawley, A., Hanson, M., Maraganore, D., Adler, C., Cookson, M.R., Muenter, M., Baptista, M., Miller, D., Blancato, J., Hardy, J., Gwinn-Hardy, K., 2003. alpha-Synuclein locus triplication causes Parkinson's disease. Science 302 (5646), 841.

Sotnikova, T.D., Beaulieu, J.M., Barak, L.S., Wetsel, W.C., Caron, M.G., Gainetdinov, R.R., 2005. Dopamine-independent locomotor actions of amphetamines in a novel acute mouse model of Parkinson disease. PLoS Biol. 3 (8), e271.

Spillantini, M.G., Crowther, R.A., Jakes, R., Hasegawa, M., Goedert, M., 1998. Alpha-synuclein in filamentous inclusions of Lewy bodies from Parkinson's disease and dementia with lewy bodies. Proc. Natl. Acad. Sci. U.S.A. 95 (11), 6469–6473.

Takeda, A., Mallory, M., Sundsmo, M., Honer, W., Hansen, L., Masliah, E., 1998. Abnormal accumulation of NACP/alpha-synuclein in neurodegenerative disorders. Am. J. Pathol. 152 (2), 367–372.

Tillerson, J.L., Caudle, W.M., Reveron, M.E., Miller, G.W., 2002. Detection of behavioral impairments correlated to neurochemical deficits in mice treated with moderate doses of 1-methyl-4-phenyl-1,2,3,6-tetrahydropyridine. Exp. Neurol. 178 (1), 80–90.

Tofaris, G.K., Garcia Reitbock, P., Humby, T., Lambourne, S.L., O'Connell, M., Ghetti, B., Gossage, H., Emson, P.C., Wilkinson, L.S., Goedert, M., Spillantini, M.G., 2006. Pathological changes in dopaminergic nerve cells of the substantia nigra and olfactory bulb in mice transgenic for truncated human alpha-synuclein(1–120): implications for Lewy body disorders. J. Neurosci. 26 (15), 3942–3950.

Tofaris, G.K., Razzaq, A., Ghetti, B., Lilley, K.S., Spillantini, M.G., 2003. Ubiquitination of alpha-synuclein in Lewy bodies is a pathological event not associated with impairment of proteasome function. J. Biol. Chem. 278 (45), 44405–44411.

Ueda, K., Fukushima, H., Masliah, E., Xia, Y., Iwai, A., Yoshimoto, M., Otero, D.A., Kondo, J., Ihara, Y., Saitoh, T., 1993. Molecular cloning of cDNA encoding an unrecognized component of amyloid in Alzheimer disease. Proc. Natl. Acad. Sci. U.S.A. 90 (23), 11282–11286.

van der Putten, H., Wiederhold, K.H., Probst, A., Barbieri, S., Mistl, C., Danner, S., Kauffmann, S., Hofele, K., Spooren, W.P., Ruegg, M.A., Lin, S., Caroni, P., Sommer, B., Tolnay, M., Bilbe, G., 2000. Neuropathology in mice expressing human alpha-synuclein. J. Neurosci. 20 (16), 6021–6029.

Vila, M., Jackson-Lewis, V., Guegan, C., Wu, D.C., Teismann, P., Choi, D.K., Tieu, K., Przedborski, S., 2001. The role of glial cells in Parkinson's disease. Curr. Opin. Neurol. 14 (4), 483–489.

Vincent, S., Marty, L., Fort, P., 1993. S26 ribosomal protein RNA: an invariant control for gene regulation experiments in eucaryotic cells and tissues. Nucleic Acids Res. 21 (6), 1498.

Wakabayashi, K., Hayashi, S., Yoshimoto, M., Kudo, H., Takahashi, H., 2000. NACP/alpha-synuclein-positive filamentous inclusions in astrocytes and oligodendrocytes of Parkinson's disease brains. Acta Neuropathol. (Berl.) 99 (1), 14–20.

Wakabayashi, K., Matsumoto, K., Takayama, K., Yoshimoto, M., Takahashi, H., 1997. NACP, a presynaptic protein, immunoreactivity in Lewy bodies in Parkinson's disease. Neurosci. Lett. 239 (1), 45–48.

Zarranz, J.J., Alegre, J., Gomez-Esteban, J.C., Lezcano, E., Ros, R., Ampuero, I., Vidal, L., Hoenicka, J., Rodriguez, O., Atares, B., Llorens, V., Gomez Tortosa, E., del Ser, T., Munoz, D.G., de Yebenes, J.G., 2004. The new mutation, E46K, of alpha-synuclein causes Parkinson and Lewy body dementia. Ann. Neurol. 55 (2), 164–173.

OPEN ACCESS Freely available online PLoS one

Ablation of NMDA Receptors Enhances the Excitability of Hippocampal CA3 Neurons

Fumiaki Fukushima[1], Kazuhito Nakao[1], Toru Shinoe[2¤a], Masahiro Fukaya[3], Shin-ichi Muramatsu[4], Kenji Sakimura[5], Hirotaka Kataoka[1], Hisashi Mori[1¤b], Masahiko Watanabe[3], Toshiya Manabe[2,6], Masayoshi Mishina[1]*

1 Department of Molecular Neurobiology and Pharmacology, Graduate School of Medicine, University of Tokyo, Tokyo, Japan, 2 Division of Neuronal Network, Institute of Medical Science, University of Tokyo, Tokyo, Japan, 3 Department of Anatomy, Hokkaido University School of Medicine, Sapporo, Japan, 4 Division of Neurology, Department of Medicine, Jichi Medical University, Tochigi, Japan, 5 Department of Cellular Neurobiology, Brain Research Institute, Niigata University, Niigata, Japan, 6 CREST, JST, Kawaguchi, Japan

Abstract

Synchronized discharges in the hippocampal CA3 recurrent network are supposed to underlie network oscillations, memory formation and seizure generation. In the hippocampal CA3 network, NMDA receptors are abundant at the recurrent synapses but scarce at the mossy fiber synapses. We generated mutant mice in which NMDA receptors were abolished in hippocampal CA3 pyramidal neurons by postnatal day 14. The histological and cytological organizations of the hippocampal CA3 region were indistinguishable between control and mutant mice. We found that mutant mice lacking NMDA receptors selectively in CA3 pyramidal neurons became more susceptible to kainate-induced seizures. Consistently, mutant mice showed characteristic large EEG spikes associated with multiple unit activities (MUA), suggesting enhanced synchronous firing of CA3 neurons. The electrophysiological balance between fast excitatory and inhibitory synaptic transmission was comparable between control and mutant pyramidal neurons in the hippocampal CA3 region, while the NMDA receptor-slow AHP coupling was diminished in the mutant neurons. In the adult brain, inducible ablation of NMDA receptors in the hippocampal CA3 region by the viral expression vector for Cre recombinase also induced similar large EEG spikes. Furthermore, pharmacological blockade of CA3 NMDA receptors enhanced the susceptibility to kainate-induced seizures. These results raise an intriguing possibility that hippocampal CA3 NMDA receptors may suppress the excitability of the recurrent network as a whole *in vivo* by restricting synchronous firing of CA3 neurons.

Citation: Fukushima F, Nakao K, Shinoe T, Fukaya M, Muramatsu S-i, et al. (2009) Ablation of NMDA Receptors Enhances the Excitability of Hippocampal CA3 Neurons. PLoS ONE 4(1): e3993. doi:10.1371/journal.pone.0003993

Editor: Frederic Andre Meunier, The University of Queensland, Australia

Received September 4, 2008; **Accepted** December 3, 2008; **Published** January 14, 2009

Funding: This work was supported in part by Grant-in-Aid for Scientific Research on Priority Areas (Molecular Brain Science) and Global COE Program (Integrative Life Science Based on the Study of Biosignaling Mechanisms) from the Ministry of Education, Culture, Sports, Science and Technology of Japan. F.F. was supported by Japan Society for the Promotion of Science, and S.T. by the 21st Century COE Program, the Ministry of Education, Culture, Sports, Science and Technology of Japan. The funders had no role in study design, data collection and analysis, decision to publish, or preparation of the manuscript.

Competing Interests: The authors have declared that no competing interests exist.

* E-mail: mishina@m.u-tokyo.ac.jp

¤a Current address: Division of Molecular and Developmental Biology, Institute of Medical Science, University of Tokyo, Tokyo, Japan,
¤b Current address: Department of Molecular Neuroscience and Pharmaceutical Sciences, Graduate School of Medicine, University of Toyama, Toyama, Japan

Introduction

Hippocampal CA3 pyramidal neurons form abundant recurrent connections with other CA3 neurons [1,2]. The activity of single pyramidal neurons spreads to other CA3 neurons and this facilitates the rapid synchronization of action-potential firing in CA3 neurons [3]. Synchronized discharges of hippocampal CA3 neurons are supposed to underlie network oscillations [4], memory consolidation [5] and seizure generation [6]. Physiological sharp wave (SPW) activity that occurs during slow-wave sleep and behavioral immobility is dependent on synchronous discharges by population of CA3 pyramidal neurons [7,8]. Synchronized CA3 activity may also contribute to the pathological EEG pattern, known as an interictal spike, which indicates a propensity for temporal lobe seizures [6].

NMDA receptors play key roles in synaptic plasticity and memory [9]. In the CA3 network, NMDA receptors are abundant at the commissural/associational synapses but scarce at the mossy fiber synapses [10]. Thus, the CA3 recurrent network is under the control of NMDA receptors. NMDA receptors in the hippocampal CA3 region are implied in rapid acquisition and recall of associative memory as well as paired associate learning [11–13]. On the other hand, studies with hippocampal slices showed that the synchronous network activity induces NMDA receptor-dependent LTP of CA3 recurrent synapses [14] and that stimuli that induced NMDA receptor-dependent LTP in the CA3 region generated sharp wave-like synchronous network activity [15]. These *in vitro* observations raised the hypothesis that the NMDA receptor-mediated LTP contributes to the generation of synchronous network activity. Here, we generated hippocampal CA3 pyramidal neuron-specific NMDA receptor mutant mice on the pure C57BL/6N genetic background. The ablation of hippocampal CA3 NMDA receptors resulted in the enhancement of the susceptibility to kainate-induced seizure and the emergence of characteristic large EEG spikes. We also showed that the virus-mediated ablation of hippocampal CA3 NMDA receptors in the

adult mice generated characteristic large EEG spikes and that pharmacological blockade of CA3 NMDA receptors enhanced the susceptibility to kainate-induced seizures. These results raise an intriguing possibility that NMDA receptors may control negatively the excitability of the hippocampal CA3 recurrent network as a whole *in vivo*.

Methods

Generation of mice

Genomic DNA carrying the exon 11 to 22 of the *GluRζ1* gene was isolated by screening a bacterial artificial chromosome (BAC) library prepared from the C57BL/6 strain (Incyte Genomics) with the 2.2 kb-*Eco*RI fragment from pBKSAζ1 [16]. The 13.3-kb *Eco*RI-*Xba*I fragment of the BAC clone was used for construction of the targeting vector. The *loxP* site was inserted into the *Bam*HI site between exon 18 and 19, and the 1.8-kb DNA fragment carrying the *loxP* sequence and *Pgk-1* promoter-driven neomycin phosphotransferase gene (*neo*) flanked by two Flp recognition target (*frt*) sites into the *Spe*I site between exon 20 and 21. Endogenous *Eco*RI site at the 5′ end of 13.3-kb *Eco*RI-*Xba*I genomic fragment was replaced with *Not*I site and an exogenous *Eco*RI site was inserted between the second *loxP* site and *neo* gene. The targeting vector pζ1TV was composed of the 14.8-kb *Not*I-*Xba*I fragment, MC1 promoter-driven diphteria toxin gene derived from pMC1DTpA and pBluescript II SK(+) [17]. The targeting vector was linearized by *Not*I and electroporated into ES cells derived from the C57BL/6N strain [18,19]. Recombinant clones were identified by Southern blot analysis of *Eco*RI-digested genomic DNA using 284-bp fragment amplified with primers 5′-ATAGAGAAAGACATGGGGC-3′ and 5′-TGCTACTGTGCAGGAAGTG-3′ from pζ1TV, the 0.6 kb *Pst*I fragment from pLFNeo [20], and the 1.1-kb *Xho*I–*Eco*RI fragment from the BAC clone as 5′ inner, neo, and 3′ outer probes, respectively. The $GluR\zeta1^{flox}$ allele was also identified by PCR using primers 5′-GCAGTGAGGCTCACACAGGCCTGAAGACTA-3′ and 5′-AGTGAACTCGGATCCTGACCATTGGCCACT-3′. Chimeric mice production and elimination of the *neo* gene from the genome through Flp/frt-mediated excision were carried out essentially as described [18–20].

GluRγ1-Cre mice were obtained by inserting the *cre* gene in the translational initiation site of the *GluRγ1* gene in frame using ES cells derived from the C57BL/6N strain [19]. The 1.8-kb DNA fragment, which carried the polyadenylation signal sequence and *pgk-1* promoter-driven *neo* gene flanked by two *frt* sites [20], was inserted into the downstream of the *cre* gene. $GluR\zeta1^{+/flox}$ mice were crossed with GluRγ1-Cre mice to yield $GluR\gamma1^{+/cre}$; $GluR\zeta1^{flox/flox}$ mice. The $GluR\gamma1^{+/cre}$ allele was identified by PCR using primers 5′-AACTGCAGTCTTGCATGCTCTCTGGAGCC-3′, 5′-GGAGCGGAGACACGGGGCAT-3′ and 5′-TTGCCCCTGTTTCACTATCC-3′. Cre recombinase-mediated NMDA receptor ablation is hippocampal CA3 pyramidal neuron-specific in $GluR\gamma1^{+/cre}$; $GluR\zeta1^{flox/flox}$ mice (Fig. 1). It is unknown why the *GluRγ1* promoter-driven Cre expression does not exactly follow the expression pattern of GluRγ1 [21]. The insertion of the *pgk-1* promoter-driven *neo* gene and the polyadenylation signal sequence together may affect the Cre expression pattern since the elimination of the *neo* gene through Flp-mediated recombination altered the expression pattern.

All animal procedures were approved by the Animal Care and the Use Committee of Graduate School of Medicine, the University of Tokyo (Approval # 1721T062). Mice were fed *ad libitum* with standard laboratory chow and water in standard animal cages under a 12 h light/dark cycle.

AAV-Cre vector

We employed AAV to deliver Cre recombinase since AAV is safe, non-pathogenic, non-inflammatory and extremely stable stable [22,23]. AAV-Cre or AAV-EGFP vector contains an expression cassette consisting of a human cytomegalovirus immediate-early promoter (CMV promoter), followed by the human growth hormone first intron, cDNA of Cre recombinase with a nuclear localization signal or the enhanced green fluorescence protein (EGFP), and simian virus 40 polyadenylation signal sequence (SV40 polyA), between the inverted terminal repeats (ITR) of the AAV-2 genome. The two helper plasmids, pAAV-RC and pHelper (Agilent Technologies, Santa Clara, California), harbor the AAV *rep* and *cap* genes, and the *E2A*, *E4*, and *VA RNA* genes of the adenovirus genome, respectively. HEK293 cells were cotransfected by the calcium phosphate coprecipitation method with the vector plasmid, pAAV-RC, and pHelper. AAV vectors were then harvested and purified by two sequential continuous iodoxale ultracentrifugations. The vector titer was determined by quantitative DNA dot-blot hybridization or quantitative PCR of DNase-I-treated vector stocks. Before administration, AAV vectors were diluted in phosphate-buffered saline to $5–8\times10^{10}$ genome copies/μl. A glass micropipette was inserted into the hippocampal CA3 region of ketamine-anesthetized mice (AP, L, V = −1.2, ±1.2, +2.0; −1.7, ±2.0, +2.1; −2.2, ±2.5, +2.4; −2.7, ±3.2, +3.5; −3.2, ±2.5, +4.0). Two minutes after the insertion, 1.0 μl of a virus solution or vehicle was injected at a constant flow rate of 16.6 nl/min, and the glass micropipette was left in this configuration for an additional 2 min, to prevent reflux of the injected material along the injection track, before being slowly retracted. AAV spread 0.5–0.7 mm both rostrodorsally and laterally. For every injected animal, the limit of the infected region was verified by immunohistochemistry for Cre recombinase or GluRζ1.

Immunological analysis

Immunohistochemistry was done as described [24] using antibodies against VGluT2 (guinea pig) [25], Calbindin (rabbit) [26], PSD-95 (rabbit) [27], GluRα1 (rabbit) [28], GAD (guinea pig) [29], and Cre recombinase (1:1000; rabbit; Novagen). Immunobloting analyses in whole-brain homogenate were carried out using antibodies for GluRζ1 (rabbit) [30], and neuron-specific enolase (1:4000; Chemicon) and chemiluminescense (Amersham Biosciences).

Golgi staining

Coronal brain sections (2 mm) were immersed for 4 days in a solution composed of 5% glutaraldehyde (Wako) and 2% $K_2Cr_2O_7$ (Sigma) and then transferred to a 0.75% solution of $AgNO_3$ (Sigma) for further 4 days. The treated brain was sectioned (100 μm), dehydrated and mounted on glass slides.

Morphology of AAV-EGFP infected CA3 neurons

AAV-EGFP vector was delivered into the hippocampal CA3 region of ketamine-anesthetized control and mutant mice of 8 weeks old. Fourteen days later, fixed coronal brain sections (150 μm) were prepared. Neurons were examined with a Leica SP-5 confocal laser scanning microscope. Optical sections were collected at intervals of 0.15 μm and averaged 16 times using a 100×objective (N.A. 1.4). The distance between axonal varicosities was measured from 50 μm-portions of CA3 axons within the CA3 stratum radiatum [31]. For spine analysis, only spines on clearly visible tertiary apical and basal branches were imaged. During the quantitation of the spine density, putative spines in the

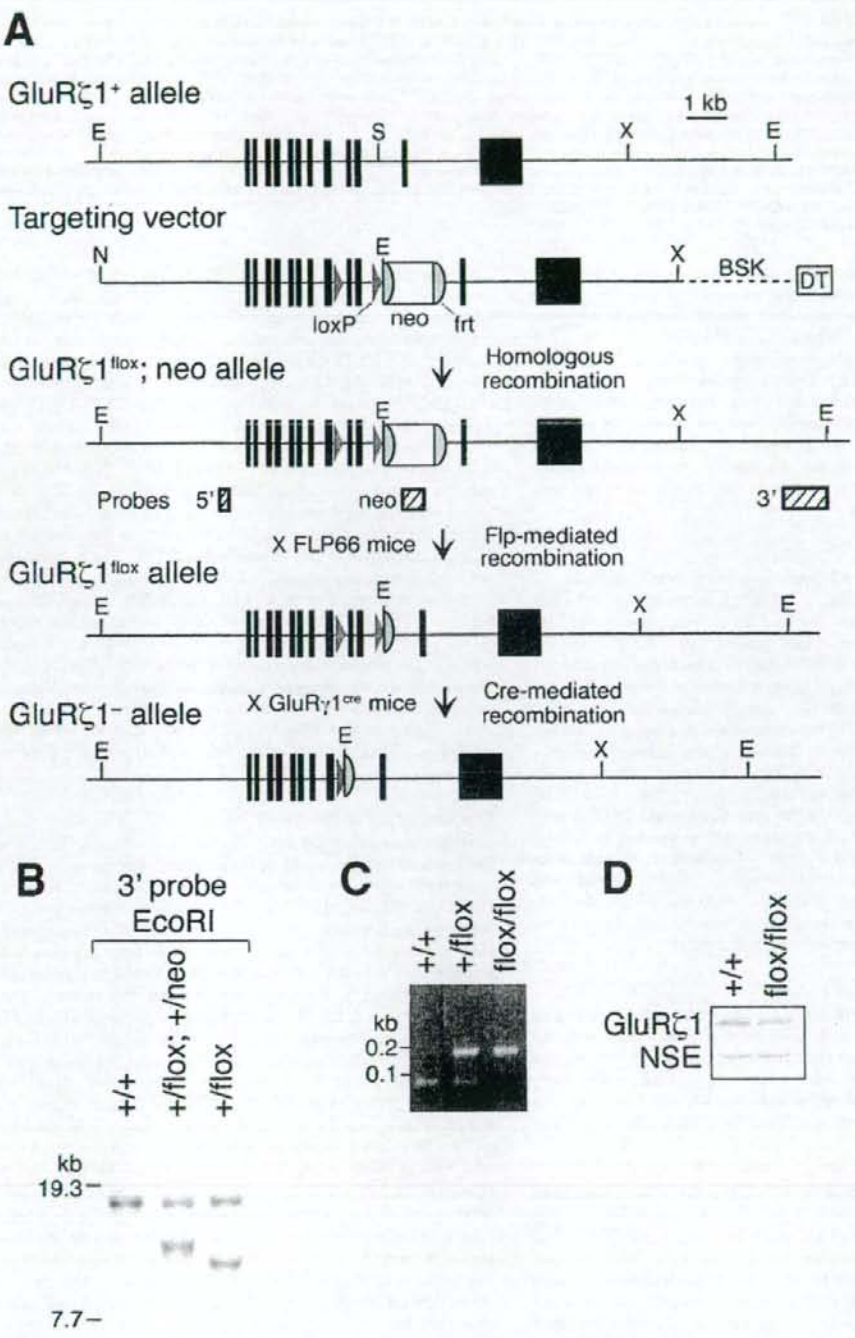
A
GluRζ1+ allele
1 kb
E
S
X
E
Targeting vector
N
E
X
BSK
DT
loxP
neo
frt
GluRζ1flox; neo allele
Homologous recombination
E
E
X
E
Probes 5'
neo
3'
X FLP66 mice
Flp-mediated recombination
GluRζ1flox allele
E
E
X
E
GluRζ1− allele
X GluRγ1cre mice
Cre-mediated recombination
E
E
X
E
B
3' probe
EcoRI
+/+
+/flox; +/neo
+/flox
kb
19.3
7.7
C
+/+
+/flox
flox/flox
kb
0.2
0.1
D
+/+
flox/flox
GluRζ1
NSE